Chemical variations of loess from the Chinese Loess Plateau and its implications

Journal:	*International Geology Review*
Manuscript ID	TIGR-2022-0038.R2
Manuscript Type:	Data Article
Date Submitted by the Author:	22-Feb-2022
Complete List of Authors:	Xiao, Yuanyuan; CAS Key Laboratory of Marine Geology and Environment, Institute of Oceanology, Chinese Academy of Sciences Huang, Zihang; CAS Key Laboratory of Marine Geology and Environment, Institute of Oceanology, Chinese Academy of Sciences, Qingdao 266071, China Sui, Peishan; CAS Key Laboratory of Marine Geology and Environment, Institute of Oceanology, Chinese Academy of Sciences Niu, Yaoling; Department of Earth Sciences, Durham University Sun, Weidong; Qingdao National Laboratory for Marine Science and Technology, Laboratory for Marine Mineral Resources; Institute of Oceanology Chinese Academy of Sciences, Center of Deep Sea Research; University of the Chinese Academy of Sciences Wang, Guo-Dong; Shandong Provincial Key Laboratory of Water and Soil Conservation and Environmental Protection, School of Resources and Environment, Linyi University Kong, Juanjuan; College of Ocean Science and Engineering, Shandong University of Science and Technology Shao, Fengli; Institute of Geology and Paleontology, Linyi University Wang, Xiaohong; CAS Key Laboratory of Marine Geology and Environment, Institute of Oceanology, Chinese Academy of Sciences Gong, Hongmei; CAS Key Laboratory of Marine Geology and Environment, Institute of Oceanology, Chinese Academy of Sciences Duan, Meng; CAS Key Laboratory of Marine Geology and Environment, Institute of Oceanology, Chinese Academy of Sciences
Keywords:	Upper continental crust, loess, Chinese Loess Plateau, elemental behaviors, carbonate

Highlights

- Fluid-soluble elements are conserved during sedimentary processes to produce loess from Chinese Loess Plateau.
- Highlight the significant contribution of carbonate for estimates of average composition of upper continental crust.
- Important updates to the loess composition and average composition of the upper continental crust.

Chemical variations of loess from the Chinese Loess Plateau and its implications

Yuanyuan Xiao[1, 2, 3, *], Zihang Huang[1, 4], Peishan Sui[1, 4], Yaoling Niu[2, 5, 6], Weidong Sun[2, 3, 7], Guodong Wang[8], Juanjuan Kong[9], Fengli Shao[10], Xiaohong Wang[1, 3], Hongmei Gong[1, 3], Meng Duan[1, 3]

1 CAS Key Laboratory of Marine Geology and Environment, Institute of Oceanology, Chinese Academy of Sciences, Qingdao 266071, China

2 Laboratory for Marine Geology, Qingdao National Laboratory for Marine Science and Technology, Qingdao 266061, China

3 Center for Ocean Mega-Science, Institute of Oceanology, Chinese Academy of Sciences

4 University of Chinese Academy of Sciences, Beijing 100049, China

5 Department of Earth Sciences, Durham University, Durham DH1 3LE, UK

6 School of Earth Science and Mineral Resources, China University of Geosciences, Beijing 100083, China

7 Center of Deep-sea Research, Institute of Oceanology, Chinese Academy of Sciences, Qingdao 266071, China

8 Shandong Provincial Key Laboratory of Water and Soil Conservation and Environmental Protection, School of Resources and Environment, Linyi University, Linyi, 276000, China

9 College of Ocean Science and Engineering, Shandong University of Science and Technology, Qingdao 266590, China

10 Institute of Geology and Paleontology, Linyi University, Linyi, 276000, China

Abstract (187 words), text (5637 words), 9 figures, 1 table, 3 tables and 2 files in the supplementary materials

*Corresponding author: Dr. Yuanyuan Xiao. E-mail: yuanyuan.xiao@qdio.ac.cn.

Abstract

Chinese Loess Plateau (CLP) is the largest loess deposit on the Earth with expansive surface-exposed source rocks of varying origin, age, and history ~~through~~ thorough mixing during long-distance transport. We present elemental abundances on representative loess and paleosol samples from seven classic sections of the CLP. Most elements, including water-soluble elements (e.g., Rb and Cs), show significant correlations with La or Al_2O_3. These correlations indicate the conservation of these elements during weathering, transport, and deposition hosted or absorbed in particle minerals (e.g., mica, K-feldspar, and clay minerals). These new observations allow the use of La/X ("X" being the element of interest), and using the widely accepted La content of 31 ppm in the model upper continental crust (UCC) to refine the UCC composition. The results show higher Cs (Cs = 6.7 ± 1.2 ppm), lower transition metals, Ba, and Ga. Given the high CaO and presence of carbonate in UCC rocks of both vast western China (the primary source for the CLP) and eastern China, we propose that these updates on the element abundances of the CLP loess represent a possibly improved model for the carbonate-bearing UCC.

Keywords: Upper continental crust; loess; Chinese Loess Plateau; elemental behaviors; carbonate

1. Introduction

The scientific significance of upper continental crust (UCC) on which we live is self-evident as it represents the surficial end-product of chemical differentiation of the Earth over its long and complex history. As the starting point to understand the formation of continental crust, geochemists have been endeavoring to estimate the average composition of continental crust, especially the UCC, using various methods over the past century. Two approaches have been commonly taken: (1) weighted averages of bedrock compositions through systematic large-scale sampling (Shaw et al., 1967; Gao et al., 1998) and (2) analyzing average compositions of fine-grained sediments or sedimentary rocks (e.g., shales) in the UCC (Condie, 1993; Chauvel et al., 2014). These methods provide good constraints on the abundances of major elements and water-insoluble minor and trace elements of the UCC. However, the abundances of transition metals and water-soluble elements have not been well constrained because of preferential/differential chemical weathering and limited analyses.

Loess, formed as the result of wind-blown silt-size particle deposition, occupies ~ 10% of the Earth's land surface (Fig. 1; Pye, 1995; Taylor et al., 1983). Because it was formed in arid and/or cold climatic conditions (i.e., peridesert loess and periglacial loess; Pye, 1995), loess has experienced physical weathering with limited chemical weathering during its transport and deposition (Gallet et al., 1998; Peucker-Ehernbrink and Jahn, 2001). Hence, loess best reflects source rock compositions with no or rather limited element fractionations. Furthermore, global loess shows similar patterns and ratios of rare earth elements (REEs) and Th (e.g., Taylor et al., 1983), which are also comparable to those of the UCC estimated by using other approaches (Fig. 2). Hence, loess can be taken as a natural mixture of materials eroded from the expansive regions of the surficial crust (Chauvel et al., 2014; Gallet et al., 1998; Taylor et al., 1983).

Previous studies, however, show that the contents of water-soluble trace elements (e.g., K, and Ba) in loess are either uncorrelated or poorly correlated with water-insoluble elements, such as La (e.g., Rudnick and Gao, 2003 and references therein), suggesting that water-soluble elements may have been differentially leached during weathering. Consequently, the contents of water-insoluble trace elements (e.g., Nb, Ta, and Th) in loess (Fig. 2a,b) are thus used to estimate the contents of water-insoluble elements in the UCC. Some other studies, however, suggest that some of the "weathering signatures" may in fact be inherited from eroded bedrocks, recording previous weathering events (e.g., Peucker-Ehernbrink and Jahn, 2001). Moreover, recent studies have also shown that loess composition can vary with varying provenances in space and time (Chen et al., 2007; Chen and Li, 2013; Nie et al., 2014; Sun et al., 2010; Sun and Zhu, 2010; Xiao et al., 2012). In addition, eroded materials may have experienced mineral sorting, which can lead to the fractionation of heavy minerals and their hosted elements (Taylor and McLennan, 1995).

Whether a chemical element in loess can be used to infer its content in the average UCC thus depends on the source inheritance and mixing processes. Therefore, a clear understanding of elemental behaviors in all aspects of sedimentary processes to produce loess is required for better constraining the average composition of the UCC using the loess composition. Compared to periglacial loess (e.g., western Europe loess, Argentinian), dust in peridesert loess was derived from different source rocks of a larger area with longer distance transport and more effective mixing (e.g., Chauvel et al., 2014). Among these peridesert loess deposits, the Chinese Loess Plateau (CLP) is the thickest and most extensive loess deposit on the Earth (e.g., Liu and Ding, 1998) with an exposure area in excess of *c*. 635,280 km^2 and thickness of up to *c*. 505 m locally (Li et al., 2020). Here, we present chemical compositions of loess samples from seven representative sections of the CLP (Fig. 1b-e), and discuss the controls on the behaviors of various elements during sedimentary processes from weathering to erosion and to deposition. This study showed that the CLP loess is an excellent candidate for estimating the average composition of the carbonate-bearing UCC for most elements, including water-soluble elements (e.g., K, Rb, Cs, Ba).

2. Samples and methods

2.1 The geological setting of the CLP and sampling sections

Aeolian dusts of the CLP are interpreted to have derived from vast arid lands upwind to the west and northwest (e.g., the Taklamakan Desert in western China, the Qaidam Gobi-Desert on the northern Tibetan Plateau, and the Badain Jaran and Tengger deserts in northern China) and originated from erosion of the surrounding mountain ranges (i.e., the Altyn mountains, Qilian mountains, and Kunlun mountains on the north edge of the Northern Tibetan Plateau, and the Tianshan mountains and

Gobi Altay mountains from the Central Asian Orogenic belt as shown in Fig. 1b; Chen et al., 2007; Chen and Li, 2013; Xiao et al., 2012). Because of the Tibetan Plateau uplift and northern hemisphere glaciation (e.g., An et al., 2001; Sun et al., 2010, 2020; Sun and Zhu, 2010), vast areas of bedrocks have been exposed for erosion to supply aeolian dusts to the CLP. Varied provenances and long-distance transport in combination facilitate effective dust mixing compared to periglacial loess (e.g., Western Europe loess; Chauvel et al., 2014; Sauzéat et al., 2015).

We sampled seven classic sections of the CLP in this study: Luochuan (6 loess samples and 5 paleosol samples), Yan'an (2 loess samples), Hukou (5 loess samples), Lingtai (4 loess samples), Lantian (3 loess samples and 2 paleosol samples), Jiuzhoutai (10 loess samples), and Qin'an (5 loess samples; Fig.1b-e). All these CLP sections are Quaternary deposits of < *c.* 2.6 Ma, but the Qin'an section that is significantly older, deposited at ~ 22–6.2 Ma as evidenced by paleomagnetic data and fossils (e.g., Guo et al., 2002). Bulk-rock loess samples were analyzed in this study to avoid artificial fractionation caused by varying grain sizes, which reflect varied sources and complex sedimentary histories.

2.2 Analytical methods

The loess samples were carefully hand-crushed in an agate mortar into powders in a clean environment for bulk-rock analysis to avoid potential contaminations. The samples were analyzed in the Laboratory of Ocean Lithosphere and Mantle Dynamics (LOLMD) in the Institute of Oceanology, the Chinese Academy of Sciences.

Inductively coupled plasma optical emission spectrometer (ICP-OES, Agilent 5100) and inductively coupled plasma mass spectrometer (ICP-MS, Agilent 7900) were used for analyzing major and trace elements, respectively. Strontium isotope compositions were measured on a multi-collector inductively coupled plasma mass spectrometer (MC-ICP-MS, Nu II). The analytical data of chemical compositions and Sr isotope compositions are given in Supplementary Table 1-3, and detailed information for analytical precision and accuracy are given in Supplementary File A.

For major elements, each dried sample powder of 50 mg mixed with 250 mg lithium borate flux ($LiBO_4$) was melted in a platinum crucible at 1050°C for 0.5 hour in a muffle furnace, followed by heating over a Bunsen burner at 1000°C. Then, the melted droplet was immediately dropped into *c.* 50 mL 5% HNO_3 solution and diluted to 100 mL with Mili-Q water (Kong et al., 2019). Our repeated analyses of United States Geological Survey (USGS) rock standards (BHVO-2, AGV-2, and GSP-2) agree with recommended values, better than 5% for accuracy and better than 3% for precision (Supplementary File A). For loss on ignition (LOI), ~ 500 mg powder for each sample was heated in a muffle furnace at 1000°C for 0.5 hours with the calculated weight loss as the LOI.

For trace element analysis, 50 mg powder for each sample was dissolved in anti-aqua regia (HNO_3 : HCl = 3:1) and HF in a high-pressure bomb (a Teflon beaker in a stainless steel jacket) for 15 hours, followed by 2 hours re-digestion with 20% HNO_3, following Chen et al. (2017). Then, each sample solution was diluted to 100g (with dilution factor of 2000) in 2% HNO_3 for analysis. During analysis, ICP-MS was settled in no gas mode instead of using collision mode, and calibration was performed based on five solutions (1, 10, 25, 50 and 100 ng/mL for all the analyzed elements) acquired from multi-element calibration standard solutions (Agilent Technologies, Tokyo, Japan) with a blank. One replicate sample was analyzed for every ten samples, and a given lab-mixed solution was analyzed every four samples to monitor instrumental drift. USGS standards (BCR-2, AGV-2, and GSP-2) were analyzed as unknowns to determine accuracy and precision (Supplementary File A). Accuracy, indicated by RE between analyzed values of USGS standards and their recommended values, is generally better than 10% for most trace elements (except for BCR-2 with 12% RE for Ni and Cu, and 15% for Sn), with many elements agreeing with the reference values within 5% (Supplementary File A). Precision, indicated by replicate analyses, is within 5% for most trace elements (Supplementary File A).

For Sr isotope analysis, 50 mg sample powder was decomposed in a high-pressure bomb by using HNO_3 + HCl + HF at 190°C for 15 hours, followed by re-digestion with 2 mL 3N HNO_3 for 2 hours. Then, sample solutions were loaded onto Sr-spec resin columns for Sr separation, and dry plasma mode with Aridus II was used for analysis. As the relative abundances of ^{83}Kr and ^{86}Kr are constant and no interference for ^{83}Kr, ^{86}Kr was calculated based on measured ^{83}Kr. The intensity of ^{86}Sr was acquired by reducing ^{86}Kr from the total measured isotope at mass 86. The measured $^{87}Sr/^{86}Sr$ ratios were normalized to $^{86}Sr/^{88}Sr = 0.11940$ to remove the effect of instrumental mass fractionation. NBS-987 was analyzed bracketing every four samples to monitor the instrument drift during the analysis. The repeated measurements of $^{87}Sr/^{86}Sr$ ratios of NBS-987 is 0.710244 ± 0.000009 (n = 9, 2σ), consistent with the reference value (0.710243 – 0.710250; http://georem.mpch-mainz.gwdg.de/sample_query_pref.asp). Analysis of BCR-2 gives $^{87}Sr/^{86}Sr$ = 0.705336 ± 0.000007, which agrees well with the recommended value of 0.70492 ± 0.00055.

For petrographic studies, mineral phases in thin sections were identified by using focused ion beam (FIB) - scanning electronic microscopy (SEM, Zeiss Gemini 2 crossbeam 550) with energy dispersive spectrometer (EDS, Bruker QUANTAX) at China University of Petroleum (East China). To determine mineral modal abundances, advanced mineral identification and characterization system (AMICS) software was used.

3. Results

3.1 Mineral counting results

The back-scattered images and mineral modal abundances acquired using SEM-EDS with AMICS are shown in Fig. 3. The mineralogy of the CLP loess and paleosol is primarily composed of quartz + feldspar (albite, K-feldspar and albite-anorthite) + carbonate + micas (both biotite and muscovite) + epidote with allanite + clay minerals (illite, kaolinite and chlorite). Heavy minerals include amphibole, augite, garnet, rutile, titanite, apatite and Fe-oxides. These mineral assemblages we obtained in the CLP loess confirm previous petrographic studies, in which all these minerals are reported either as single particles or parts of rock fragments in the CLP loess (Jeong et al., 2008, 2011). Ca-carbonate minerals are common in the loess, and can reach up to *c.* 40 wt.% (16QA-02) in the Qin'an section. Carbonate mainly occurs as detrital grains, evidenced by its morphology as single angular particles or as parts of rock fragments, together with some secondary carbonate (also see Supplementary File B). In comparison, the paleosols have little carbonate and much less ~~epidotite~~ epidote group minerals, but more clays (Fig. 3).

3.2 Major elements

For both the CLP loess and paleosol samples, Al_2O_3 shows negative correlations with CaO and positive correlations with TiO_2–FeOT–K_2O–MnO (Fig. 4a-e). CaO and LOI are positive correlated (Fig. 4f), reflecting that the determined LOI largely results from carbonate decomposition. Compared with the Quaternary loess samples, the Qin'an loess samples have higher CaO–LOI (up to 22.40 wt.% CaO and 21.27 wt.% LOI) and lower contents of other major elements, while paleosol samples have obviously lower CaO–LOI–Na_2O–P_2O_5 and higher SiO_2–TiO_2–Al_2O_3–Fe_2O_3–K_2O (Fig. 4 and Supplementary Table 1).

3.3 Trace elements

All the CLP loess and paleosol samples show a uniform trace element pattern (Fig. 2c,d), i.e., elevated Ba–Rb–Cs–Th–U–Pb–LREEs, low Nb–Ta–Sr, a clear negative Eu anomaly (i.e., $Eu_N/Eu* = Eu_N/(Sm*Gd)^{1/2} \approx 0.6$), and a flat HREE pattern. This pattern is similar to that of loess samples elsewhere reported in the literature, except that we do not see large positive Zr–Hf anomalies in the CLP loess and paleosol samples (Fig. 2c,d). Most analyzed elements of the CLP Quaternary loess samples show positive correlations with La (Figs. 5a-k&6a-f), including both water-soluble elements (e.g., Rb–Cs–Ba–Pb) and insoluble elements (i.e., REE and Ti–Nb–Ta–Th). However, it lacks significant correlations with Zr or Hf with the increase of La (Fig. 5l). Strontium shows a positive correlation with CaO but not with others. In addition, Molybdenum and U show scattered positive correlations (Fig. 5p), but they show no correlation with any other incompatible elements. Trace element contents of Qin'an loess samples are generally comparable with or lower than those of the CLP Quaternary loess, except for higher Sr, while the paleosols have comparable or higher contents of most trace elements except for lower Sr (Figs. 5-7 and Supplementary Table 1). Ratios of Nb/Ta (*c.* 13) and Zr/Hf (*c.* 38) of all our analyzed CLP loess and paleosol samples remain constant (Fig. 5m,n).

3.4 Strontium isotope ratios

Strontium isotope data for the CLP loess and paleosols are given in Supplementary Table 2. The $^{87}Sr/^{86}Sr$ ratios range from 0.712474 to 0.71905, which increases with increasing $^{87}Rb/^{86}Sr$ ratios (Fig. 7c). The CLP Quaternary loess has generally higher $^{87}Sr/^{86}Sr$ ratios than those of the Qin'an loess, and paleosol shows the highest $^{87}Sr/^{86}Sr$ ratios (Fig. 7c-e).

4. Compositional variations of the CLP loess and paleosol

4.1 Inheritance of carbonate minerals

The correlations between major element contents and mineral modal abundances (Fig.4g-i) suggest that the mineralogy controls on the bulk-rock variations of major element contents in the CLP loess and paleosol. As shown in Fig. 3 and Supplementary File B, carbonate minerals are important constituents of the CLP loess, which has also been reported in other CLP sections (e.g., Jeong et al., 2008, 2011). Together with the variably high CaO and LOI and their positive correlation (Fig. 4f), the significant correlation of carbonate with CaO and LOI (Fig. 4g,h) demonstrate that calcite, not dolomite (as there is no correlation with Mg), is a significant constituent of the CLP loess and controls. Furthermore, CaO and LOI do not correlate with any other element, except for Sr. As shown in Figs. 4g&7a, it is the carbonate modes that control the abundances of CaO and Sr as well as Rb/Sr ratios.

Aluminum has the lowest water-rock partition coefficient compared with other major elements during chemical weathering and can be inherited from source rocks through the transformation of feldspar to clay minerals (such as illite and kaolinite). Thus, Al_2O_3 has been taken as the constant index and its relationship with other elements has been used to identify the mobility/immobility of these elements during sedimentary processes (e.g., Taylor et al., 1983). The positive correlations of Al_2O_3 with SiO_2–TiO_2–K_2O–FeOT–MnO (Fig. 4) indicate the controls of silicate minerals (e.g., quartz, feldspar, and phyllosilicate minerals) on the varying SiO_2–TiO_2–K_2O–

FeOT–MnO abundances. Together with the negative correlations of Al_2O_3 with CaO–LOI (e.g., Fig. 4a), it reflects the complementary modal relationship between calcite and silicate minerals in the CLP loess and paleosols (i.e., the more calcite, the less silicate minerals, and vice versa).

Because carbonate minerals mainly occur as detrital grains indicated by its morphology (Fig. 3 and Supplementary File B), they are most likely derived from the provenance. Thus, the common presence of carbonate reflects the inherited signatures of high modes of carbonate and high CaO of source rocks rather than the influence by post depositional processes. Considering that both periglacial and peridesert loess are the product of an arid environment, rainfall cannot supply sufficient CaO for the precipitation of abundant carbonate in the CLP loess. Even if there were secondary carbonate minerals formed after loess deposition, they are likely re-precipitated following the dissolution of local primary carbonate, which is still of provenance origin. Hence, the common presence of calcite and high CaO–LOI in the CLP loess are most likely inherited from the provenance, which is dominated by siliciclastic and carbonate sedimentary rocks, granitoids, and their metamorphic equivalents (Jeong et al., 2008). Thus, our bulk-rock analysis without prior chemical leaching is critically important in revealing the “true” compositional makeup of the CLP loess.

4.2 ~~The~~ compositional variations

4.2.1 ~~The~~ compositional inheritance

Most of the analyzed elements, including REEs–Th, Nb–Ta, transition metals and

Ga–Sn, show significant correlations with La (Figs. 2b, 5a-k&6a-f). These correlations reflect the inheritance of these elements from the source rocks with limited chemical alterations during loess formation. The relatively constant Zr-Hf content with La is probably caused by differential physical separation of zircons (and possibly other heavy minerals; Fig. 5l). As previous studies reported for various minerals in river sediments (e.g., Garçon et al. 2014), epidote group minerals (epidote, allanite, zoisite), titanite and clay minerals are significant for hosting REEs and Th; zircon and garnet are important hosts for HREEs, while zircon, rutile, and titanite are hosts for HFSEs (Supplementary File B).

For water-soluble elements, previous studies only showed good correlations of Li with LREEs in loess (Sauzéat et al., 2015). However, this study shows that water-soluble elements (i.e., Cs-Rb-Ba-K) of loess are also significantly correlated with La ~~in this study~~ except Li (Fig. 6). These correlations indicate the conservation of these water-soluble elements during sedimentary processes to produce loess. Furthermore, the correlations of total modal abundance of micas, K-feldspar and clay minerals with Cs-Rb-Ba-K-Li (Figs. 4i&6g,h) reflect the accommodation of these elements by micas, K-feldspar and clay minerals in the loess, the latter of which may inherit from the weathered source rocks. Because different trace elements are preferentially hosted in different minerals, the conservation of important mineral hosts during sedimentary processes as single particles or rock fragments is important to preserve geochemical signatures of the provenance.

Molybdenum and U are correlated (Fig. 5p), but do not correlate with any other elements. Moreover, in contrast to the constant Th/Nb ratio, Th/U ratios of the CLP loess vary significantly from 2.5 to 5.3 with an average value of 4.0 (Fig. 5o). Given the insignificant chemical weathering under cold and arid conditions during sedimentary processes to produce loess, the variations of Mo and U may inherit geochemical signatures of bedrocks caused by previous weathering history. Because both Mo and U are sensitive to oxidation, this suggests that the source rocks may have suffered significant oxidation. As Carpentier et al. (2013) suggested, higher Th/U ratios of sediments derived from mature continental areas than those from juvenile terranes reflect the loss of U resulting from the long-term weathering history of source materials.

4.2.2 The effects of chemical alterations on paleosol

Although paleosol shows similar correlations between various elements like the loess, the paleosol is characterized by less carbonate with more clay minerals (Fig. 3), lower CaO-Na_2O-P_2O_5-LOI-Sr (Fig. 4) and higher $^{87}Sr/^{86}Sr$ ratios (Fig. 7c-e) relative to the loess.

Paleosol is thought to have experienced stronger chemical weathering and biological alterations than loess. By using the approach of McLennan (1993) to calculate values of the chemical index of alteration (CIA = 100 * molar $Al_2O_3/[Al_2O_3 + CaO^* + K_2O + Na_2O]$, and CaO^* is corrected for apatite and carbonate), paleosol has higher CIA with an average of 64 than those of the CLP loess (i.e., 58 and 61 for average CLP Quaternary loess and Qin'an loess, respectively). The stronger weathering of the paleosol, as indicated by its higher CIA values, can result in leaching and is responsible for subsequent reprecipitation of calcite at the base of the CLP paleosol (e.g., Jahn et al., 2001). Hence, the lower CaO-LOI–Sr contents of the paleosol reflect the loss of these elements caused by carbonate dissolution during pedogenisis, which can also result in a high Rb/Sr ratio and higher $^{87}Sr/^{86}Sr$ ratios (Fig. 7). In addition, the paleosol lacks correlations of Na_2O and P_2O_5 with any other elements, except scattered negative trends with Al_2O_3. Together with lower Na_2O and P_2O_5 contents in the paleosol, it indicates the loss of Na and P during post depositional weathering process, and P is also possibly ~~taken away by vegetations.~~

4.3 Temporal variations of the CLP loess

Compared to the CLP Quaternary sections, the Qin'an loess ~~has~~ originated from the large arid area in the Asian interior during the Early Miocene (e.g., Guo et al., 2002). Hence, the Qin'an and Quaternary sections offer the opportunity to determine if there may be any difference between CLP Miocene and Quaternary loess in terms of their dust sources as possible responses to tectonic and climate changes.

The Qin'an loess has higher CIA values than the Quaternary loess (i.e., 61 vs. 58 on average), indicating a stronger degree of chemical weathering. It also has abundances of most elements (i.e., SiO_2–TiO_2–Al_2O_3–Fe_2O_3–alkali elements–Ba–Pb–REEs–HFSEs–transition metals) comparable with or lower than those of the Quaternary loess, but ha~~ve~~ higher LOI–CaO–Sr (Figs. 4–7). This is consistent with petrographically observed higher proportions of carbonate that dilutes the silicate constituents in the Qin'an loess. The well-defined linear correlation of $^{87}Sr/^{86}Sr$ with

$^{87}Rb/^{86}Sr$ also reflects a clear two-component mixing relationship for both Quaternary Loess and the older Qin'an loess (Fig. 7c). The radiogenic ingrowth is a function of Rb/Sr ratios, which decrease with increasing carbonate component and with the decreasing total modal abundance of micas + clay minerals + K-feldspar. Hence, lower $^{87}Sr/^{86}Sr$ ratios of the Qin'an loess compared to Quaternary loess are attributed to more carbonate and less micas + clay minerals + K-feldspar (Fig. 7d, e).

The silicate components of the Qin'an loess also differ from those of the CLP Quaternary loess as indicated by different slopes in element covariation diagrams (Figs. 5 & 6). The significantly lower Rb relative to the difference of Sr reflects that the silicate component of Qin'an loess has lower Rb/Sr ratios and incompatible elements than Quaternary loess (Fig. 7f,g). Previous studies have also found ~~the~~ systematic differences ~~of~~ Sr-Nd-Pb-O isotopic and chemical compositions in silicate fractions after removing carbonate ~~between those~~ from Miocene loess and Quaternary loess (Chen and Li, 2013; Sun and Zhu, 2010; Sun et al., 2020).

Moreover, although the pseudochron ages have no chronological significance for the loess deposition, this study gives an older pseudochron age of the Qin'an loess than the Quaternary loess, i.e., 352 vs. 246 Ma (Fig. 7c). All these variations can be attributed to the change of the source material contribution, which is as the function of tectonic uplift and climate change (An et al., 2001; Chen and Li, 2013; Sun and Zhu, 2010; Sun et al., 2010, 2020).

5. Representativeness of the CLP loess about the UCC composition

Unlike large-scale surface sampling of shields or orogens, fine-grained terrigenous sediments can supply the naturally well-mixed composition of eroded surfaces, eliminating the deviation caused by biased sampling or weighted averaging that may plague surface sampling (e.g., Condie, 1993). Among fine-grained terrigenous sediments (e.g., shales), loess, especially that of peridesert origin, is an excellent candidate to estimate the average UCC composition, because of ignorable chemical weathering and ~~a~~ relatively long-distance transport from large source areas. It has been shown that the CLP loess deposits are the thickest and most extensive loess deposit on Earth, and the volume of dust eroded in total can be up to 190,584 km^3 given a thickness of 300 m (Li et al., 2020). Moreover, as source regions of the CLP, bedrocks of surrounding deserts (Taklamakan, Gobi, Badain Jaran and Tengger) and mountains (Altyn, Qilian, Kunlun, Tianshan and Gobi Altay; Fig. 1b), covering over 2 million square kilometers, ~~can be dated back~~ from Archean to Cenozoic (e.g., Nie et al., 2014). Hence, the CLP loess is better representative for estimating the average UCC composition than other loess deposits (e.g., Chauvel et al., 2014; Sauzéat et al., 2015).

To estimate the UCC composition, we used 30 CLP Quaternary loess samples in this study. For those elements that were also reported by Chauvel et al. (2014; everything except Be-Ga-Mo-Sn-Tm-W), we also combined their data for 13 CLP loess samples with the data reported here to estimate the average composition of the UCC (Table 1). We did not use paleosol samples because of the potential alteration associated with pedogenesis, such as the Sr loss in paleosol as mentioned above. The Miocene Qin'an loess is also excluded to better constrain the UCC composition because of different correlations of various elements with La (Figs. 5-7) and stronger effects of chemical weathering as indicated by their higher CIA values.

5.1 Major elements

The average contents of major elements of the CLP Quaternary loess agree well with recommended values of the average UCC composition (Rudnick and Gao, 2003) within ± 20% variation (Fig. 8a; Table 1) except for higher CaO and lower Na_2O, the latter of which reflects the loss of Na during the sedimentary processes as discussed above. As this study and many others (e.g., Jeong et al., 2008, 2011) have shown that abundant carbonate in the CLP loess is inherited from the provenances, high CaO contents of the CLP loess reflect the well-mixed composition of exposed surfaces upwind to the west and northwest of the CLP. Gao et al. (1998) also identified higher CaO contents and more abundant carbonate in their estimates based on large-scale sampling of eastern China (up to *c*. 8 wt.% for the interior of the North China craton) than those estimates using exposed rocks from shields (Gao et al., 1998; Rudnick and Gao, 2003). Moreover, the loess from Kaiserstuhl, Rhine Valley has much higher CaO contents, up to *c*. 23 wt.%, which reflects the presence of abundant limestone from the Alps (Hu and Gao, 2008; Taylor et al., 1983). Hence, loess compositions of the CLP and Kaiserstuhl, together with large-scale exposed bedrocks in eastern China, may represent a carbonate-bearing model of the UCC composition.

Previous studies suggested that loess had much higher SiO_2 than the model UCC composition by using the approach of large-scale surface sampling (e.g., Gallet et al., 406 1998; Taylor et al., 1983) because of preferential transport of quartz into loess and its preservation during sedimentary recycling processes (e.g., Taylor et al., 1983; Rudnick and Gao, 2003). However, our study demonstrates that averaged contents of most major elements in carbonate-rich CLP loess are comparable with the proposed UCC composition including SiO_2 (Fig. 8a). As the previous study discussed (Liang et al., 2009), removing the present carbonate in the CLP loess can lead to a ~ 3% difference for Al_2O_3 content between the carbonate-leached CLP loess and those without leaching. Hence, the presence of carbonate dilutes the contents of most major elements in the CLP loess.

5.2 Trace elements

Although loess is accepted to have experienced limited chemical alteration, most water-soluble elements are known to poorly correlate with La in loess, which may reflect the heterogeneous composition of source rocks after ~~an~~ ineffective mixing (Fig. 9a). Hence, previous studies indirectly used surface composites or used element ratios to estimate contents of these elements in the UCC (e.g., Rudnick and Gao, 2003 and references therein). However, we find significant correlations of Li-Be-K-Rb-Cs-Ba-Pb with La and Al_2O_3 in CLP loess (Figs. 4d&6), demonstrating that these elements are ~~congruently~~ transported from source rocks to loess, which allow us to update recommended values of these elements in the model UCC composition.

Given the correlations of different elements with La (Figs. 5-6) and the widely accepted La content of 31 ppm in the UCC (Rudnick and Gao, 2003), we ~~thus~~ use the average La/X ratios (McLennan, 2001; X = contents of the element of interest) to determine X as the value in the UCC (Table 1). The estimates for most trace elements in the mean UCC composition agree well with recommended values of the average UCC composition (Rudnick and Gao, 2003) within ± 20% variation (Fig. 8b; Table 1). Several elements not within uncertainty of the recommended value of Rudnick and Gao (2003, those in bracket) are as follows: ***Li*** = 34 ± 5 ppm (vs. 24 ppm), ***Cs*** = 6.7 ± 1.2 ppm (vs. 4.9 ppm), ***Ba*** = 461 ± 51 ppm (vs. 628 ppm), ***Sc*** = 11 ± 1 ppm (vs. 14 ppm) , ***V*** = 75 ± 11 ppm (vs. 97 ppm), ***Cr*** = 64 ± 7 ppm (vs. 92 ppm), ***Co*** = 11 ± 2 ppm (vs. 17 ppm), ***Ni*** = 29 ± 4 ppm (vs. 47 ppm), ***Cu*** = 21 ± 4 ppm (vs. 28 ppm), and ***Ga*** = 14 ± 2 ppm (vs. 17.5 ppm).

Although the ***Li*** value in this study is higher than recommended values (18 – 24 ppm) of Rudnick and Gao (2003 and references therein), it is identical to the values derived in recent studies, i.e., 35 ± 11 ppm based on correlations between Li and Nb in shales using MC-ICP-MS (Teng et al., 2004), 31 ± 5.2 ppm based on Neoproterozoic and Phanerozoic glacial diamictites (Gaschnig et al.2016) and comparable with the value of 30.5 ± 3.6 ppm using correlations of Li with REEs in the recent loess study by Sauzéat et al. (2015). Based on the correlation of Li with In in well-characterized UCC samples (shales, pelites, loess, graywackes, granitoids and their composites), Hu and Gao (2008) also provided a higher recommended Li value of 41 ppm.

Our ***Cs*** value is also higher than most previous estimates (Fig. 9b), except for the value of 6 ppm estimated by using sedimentary rocks (McDonough et al., 1992) and

7.3 ppm for marine sediments (Plank and Langmuir, 1998). However, this value is comparable with that of loess from the CLP and Tadjikistan (Supplementary Table 3; Chauvel et al., 2014; Hu and Gao, 2008). Of the previous studies, Cs concentrations of shield composites were only given by Gao et al. (1998; 3.6 ppm). However, because of the absence of significant correlations between Cs and La in sedimentary rocks, previous estimates ~~on~~ Cs primarily relied on the correlation of Cs with Rb and used the average Rb/Cs ratio, which is calculated assuming a concentration of Rb. The proposed values of Rb can range from 82 to 112 ppm in previous estimates (Hu and Gao, 2008; Rudnick and Gao, 2003 and references therein), and Rb/Cs ratios used also vary from 15.3 (Plank and Langmuir, 1998) to 30 (Taylor and McLennan, 1985), leading to a highly variable Cs estimate (Rudnick and Gao, 2003). Therefore, this study, based on the significant correlation of Cs with La, potentially yields a more reliable value for Cs in the UCC.

Our ***Ba*** value is lower than previous estimates (Table 1 and Fig. 9b). Because of the significant correlations between Ba–Rb–Cs–K and their correlations with La (Fig. 6), we suggest that Ba, like the alkali elements, is greatly conserved during sedimentary processes. Hence, given the comparable or considerably higher Rb and Cs contents of the CLP loess relative to their recommended values in the UCC, the lower Ba content should reflect the source rock composition. Based on the loess data of Chauvel et al. (2014), McLennan (2001), and Taylor et al. (1983), the Ba content is highly variable among different loess deposits (*c.* 190 ppm in Kaiserstuhl to *c.* 810 ppm in Iowa; Supplementary Table 3). However, because the CLP and Tadjikistan loess as important peridesert loess deposits originated from more expansive surface bedrocks (e.g., Chauvel et al., 2014), the consistently lower Ba contents of the loess from these two deposits may be more representative ~~for~~ Ba in the UCC.

The values of ***Sc–V–Cr–Co–Ni–Cu*** are lower than the values recommended by Rudnick and Gao (2003) and Taylor and McLennan (1985, 1995), but are generally consistent with those of carbonate-bearing composite by Gao et al. (1998) and those of Gaschnig et al. (2016), which are also comparable with the values of Hu and Gao (2008), except for obviously higher V (see Table 1). The values of Sc, V, and Co are also similar to those of the Canadian Shield (Eade and Fahrig, 1973; Shaw et al., 1967, 1976; Table 1). Transition metals are thought to be hosted in mafic minerals, which are preferentially incorporated into the fine-grained sediments (Garçon et al., 2014). However, the significant correlations of these elements with La support that the lower contents of these elements are inherited from their source rocks. Our ***Ga*** value is comparable with the reported Ga contents of global loess (except Kaiserstuhl with a lower Ga of *c.* 7 ppm; Hu and Gao, 2008) and with the recommended value of 14 ppm in the UCC by Wedepohl (1995), which adopted the value of Shaw et al. (1967) but is much lower than most other recommended values (Gao et al., 1998; Gaschnig et al., 2016; Hu and Gao, 2008; Rudnick and Gao, 2003; Taylor and McLennan, 1985, 1995).

6. Conclusions

This study presents chemical compositional data for the CLP loess, which ~~is~~ originated from expansive source regions with long geological histories involving multiple sedimentary cycling, long-distance transport, and effective mixing. Given the high CaO and presence of carbonate in UCC rocks ~~of~~ both vast western China (the primary source for the CLP) and eastern China, we propose that the CLP composition represents a possibly improved model for the carbonate-bearing UCC. This study also shows significant correlations for most elements (even water-soluble elements) with La and Al_2O_3, indicating that most elements are conserved during the sedimentary processes that produce the CLP loess. Therefore, the ratios of La/X can provide better constraints on element values of the average UCC. The results show higher Cs (Cs = 6.7 ± 1.2 ppm), lower transition metals, Ba, and Ga. These updates on the element abundances of the CLP loess represent a possibly improved model for the carbonate-bearing UCC.

Declaration of interests

The authors declare that they have no known competing financial interests or personal relationships that could have appeared to influence the work reported in this paper.

Acknowledgments

This paper is dedicated to the late Prof. Shan Gao, who has made major contributions to constrain the composition of the UCC. This study was supported by the National Natural Science Foundation of China (Grant numbers: 41776069 to Yuanyuan Xiao), Special project of strategic leading science and technology of Chinese Academy of Sciences (Grant number: XDB42020302). We thank the suggestion by editor Dr. Robert J. Stern and the useful discussion with Prof. Yong-Fei Zheng. We also thank Dong Wang for sample preparation and Kelai Xi and Chunyu Li for SEM-EDS analysis.

References

An, Z., Kutzbach, J.E., Prell, W.L. and Porter, S.C. (2001) Evolution of Asian monsoons and phased uplift of the Himalaya-Tibetan plateau since Late Miocene times. Nature 411, 62-66.

Carpentier, M., Weis, D. and Chauvel, C. (2013) Large U loss during weathering of upper continental crust: The sedimentary record. Chemical Geology 340, 91-104.

Chauvel, C., Garçon, M., Bureau, S., Besnault, A., Jahn, B.-m. and Ding, Z. (2014) Constraints from loess on the Hf–Nd isotopic composition of the upper continental crust. Earth and Planetary Science Letters 388, 48-58.

Chen, J., Li, G., Yang, J., Rao, W., Lu, H., Balsam, W., Sun, Y. and Ji, J. (2007) Nd and Sr isotopic characteristics of Chinese deserts: Implications for the provenances of Asian dust. Geochimica et Cosmochimica Acta 71, 3904-3914.

Chen, Z. and Li, G. (2013) Evolving sources of eolian detritus on the Chinese Loess Plateau since early Miocene: Tectonic and climatic controls. Earth and Planetary Science Letters 371-372, 220-225.

Chen, S., Wang, X., Niu, Y., Sun, P., Duan, M., Xiao, Y., Guo, P., Gong, H., Wang, G. and Xue, Q. (2017) Simple and cost-effective methods for precise analysis of trace element abundances in geological materials with ICP-MS. Sci. Bull. 62, 277-289.

Condie, K.C. (1993) Chemical composition and evolution of the upper continental crust: Contrasting results from surface samples and shales. Chemical Geology 104, 1-37.

Eade, K.E. and Fahrig, W.F. (1973) Regional, lithological, and temporal variation in the abundances of some trace elements in the Canadian Shield. Pap. Geol. Surv. Can. 7246.

Gao, S., Luo, T.-C., Zhang, B.-R., Zhang, H.-F., Han, Y.-w., Zhao, Z.-D. and Hu, Y.-K. (1998) Chemical composition of the continental crust as revealed by studies in East China. Geochimica et Cosmochimica Acta 62, 1959-1975.

Gallet, S., Jahn, B.M., Lanoe, B.V., Dia, A. and Rossello, E. (1998) Loess geochemistry and its implications for particle origin and composition of the upper continental crust. Earth and Planetary Science Letters 156, 157-172.

Garçon, M., Chauvel, C., France-Lanord, C., Limonta, M. and Garzanti, E. (2014) Which minerals control the Nd–Hf–Sr–Pb isotopic compositions of river sediments? Chemical Geology 364, 42-55.

Gaschnig, R.M., Rudnick, R.L., McDonough, W.F., Kaufman, A.J., Valley, J.W., Hu, Z., Gao, S. and Beck, M.L. (2016) Compositional evolution of the upper continental crust through time, as constrained by ancient glacial diamictites. Geochimica et Cosmochimica Acta 186, 316-343.

Guo, Z.T., Ruddiman, W.F., Hao, Q.Z., Wu, H.B., Qiao, Y.S., Zhu, R.X., Peng, S.Z., Wei, J.J., Yuan, B.Y. and Liu, T.S. (2002) Onset of Asian desertification by 22 Myr ago inferred from loess deposits in China. Nature 416, 159-163.

Hu, Z. and Gao, S. (2008) Upper crustal abundances of trace elements: A revision and update. Chemical Geology 253, 205-221.

Jahn, B.M., Gallet, S. and Han, J.M. (2001) Geochemistry of the Xining, Xifeng and Jixian sections, Loess Plateau of China: eolian dust provenance and paleosol evolution during the last 140 ka. Chemical Geology 178, 71-94.

Jeong, G.Y., Hillier, S. and Kemp, R.A. (2008) Quantitative bulk and single-particle mineralogy of a thick Chinese loess–paleosol section: implications for loess provenance and weathering. Quaternary Science Reviews 27, 1271-1287.

Jeong, G.Y., Hillier, S. and Kemp, R.A. (2011) Changes in mineralogy of loess–paleosol sections across the Chinese Loess Plateau. Quaternary Research 75, 245-255.

Kong, J., Niu, Y., Sun, P., Xiao, Y., Guo, P., Hong, D., Zhang, Y., Shao, F., Wang, X. and Duan, M. (2019) The origin and geodynamic significance of the Mesozoic dykes in eastern continental China. Lithos 332-333, 328-339.

Li, Y., Shi, W., Aydin, A., Beroya-Eitner, M.A. and Gao, G. (2020) Loess genesis and worldwide distribution. Earth-Science Reviews 201, 102947.

Liang, M., Guo, Z., Kahmann, A.J. and Oldfield, F. (2009) Geochemical characteristics of the Miocene eolian deposits in China: Their provenance and climate implications. Geochem Geophy Geosy 10.

Liu, T., Ding, Z., 1998. Chinese loess and the paleomonsoon. Annu. Rev. Earth Planet. Sci. 26, 111-145.

McLennan, S.M. (2001) Relationships between the trace element composition of sedimentary rocks and upper continental crust. Geochemistry, Geophysics, Geosystems 2.

McLennan, S.M. (1993) Weathering and Global Denudation. The Journal of Geology 101, 295-303.

Nie, J., Peng, W., Möller, A., Song, Y., Stockli, D.F., Stevens, T., Horton, B.K., Liu, S., Bird, A., Oalmann, J., Gong, H. and Fang, X. (2014) Provenance of the upper Miocene–Pliocene Red Clay deposits of the Chinese loess plateau. Earth and Planetary Science Letters 407, 35-47.

Peucker-Ehrenbrink, B. and Jahn, B.M. (2001) Rhenium-osmium isotope systematics and platinum group element concentrations: Loess and the upper continental crust. Geochem Geophy Geosy 2, 26.

Plank, T. and Langmuir, C.H. (1998) The chemical composition of subducting sediment and its consequences for the crust and mantle. Chemical Geology 145, 325-394.

Pye, K. (1995) The nature, origin and accumulation of loess. Quaternary Science Reviews 14, 653-667.

Rudnick, R.L. and Gao, S. (2003) Composition of the Continental Crust, in: Holland, H.D., Turekian, K.K. (Eds.), Treatise on Geochemistry. Elsevier, Oxford, pp. 1-64.

Sauzéat, L., Rudnick, R.L., Chauvel, C., Garçon, M. and Tang, M. (2015) New perspectives on the Li isotopic composition of the upper continental crust and its weathering signature. Earth and Planetary Science Letters 428, 181-192.

Shaw, D.M., Reilly, G.A., Muysson, J.R., Pattenden, G.E. and Campbell, F.E. (1967) An Estimate of the Chemical Composition of the Canadian Precambrian Shield. Canadian Journal of Earth Sciences 4, 829-853.

Shaw, D.M., Dostal, J. and Keays, R.R. (1976) Additional estimates of continental surface Precambrian shield composition in Canada. Geochimica et Cosmochimica Acta 40, 73-83.

Sun, J. and Zhu, X. (2010) Temporal variations in Pb isotopes and trace element concentrations within Chinese eolian deposits during the past 8Ma: Implications for provenance change. Earth and Planetary Science Letters 290, 438-447.

Sun, S.-s. and McDonough, W.F. (1989) Chemical and isotopic systematics of oceanic basalts: implications for mantle composition and processes. Geological Society, London, Special Publications 42, 313-345.

Sun, Y., An, Z., Clemens, S.C., Bloemendal, J. and Vandenberghe, J. (2010) Seven million years of wind and precipitation variability on the Chinese Loess Plateau. Earth and Planetary Science Letters 297, 525-535.

Sun, Y., Yan, Y., Nie, J., Li, G., Shi, Z., Qiang, X., Chang, H. and An, Z. (2020) Source-to-sink fluctuations of Asian aeolian deposits since the late Oligocene. Earth-Science Reviews 200, 102963.

Taylor, S.R., McLennan, S.M. and McCulloch, M.T. (1983) Geochemistry of loess, continental crustal composition and crustal model ages. Geochimica et Cosmochimica Acta 47, 1897-1905.

Taylor, S.R. and McLennan, S.M. (1985) The Continental Crust: Its Composition and Evolution. Blackwell Scientific Publication, Carlton.

Wedepohl, K.H. (1995) The composition of the continental crust. Geochimica et Cosmochimica Acta 59, 1217-1232.

Xiao, G., Zong, K., Li, G., Hu, Z., Dupont-Nivet, G., Peng, S. and Zhang, K. (2012) Spatial and glacial-interglacial variations in provenance of the Chinese Loess Plateau. Geophysical Research Letters 39.

Figure and Table captions

Fig. 1 (a) Global distributions of loess and desert (revised after Li et al., 2020 and Chauvel et al., 2014). (b) Distribution of potential source regions for the Chinese Loess Plateau (CLP) with highlights of sampling locations in this study (b; revised after Nie et al., 2014; Sun et al., 2020). CAO – the Central Asia Orogen, NTP – the Northern Tibetan Plateau, OP – the Ordos Plateau. (c-e) Photos of loess outcrops for representative sampling localities.

Fig. 2 (a) Correlation diagram of La and Al_2O_3 contents for global loess and paleosol, compared with the recommended UCC composition (black thick cross; Rudnick and Gao, 2003). (b) Correlation diagram of La and Th contents for global loess (following Gallet et al., 1998). (c) Chondrite normalized REE patterns and (d) primitive mantle normalized trace element patterns of the CLP samples using normalization values of Sun and McDonough (1989). Model UCC compositions by Taylor and McLennan (1985, 1995) and Rudnick and Gao (2003) are plotted for comparison. The plotted data for global loess and paleosol in the literature are compiled in Supplementary Table 3.

Fig. 3 Backscattered electron images and corresponding identification results of different mineral phases with their counting results by using SEM-EDS with AMICS for representative loess and paleosol samples from CLP.

Fig. 4 Correlation diagrams of major elements and LOI (a-f) and their correlations with mineral modal abundances (g-i) for loess and paleosol samples from the CLP. Major element contents shown in (a-e) have been recalculated following a sum of major elements to be 100% for comparison with the recommended UCC composition of Rudnick and Gao (2003), as shown by thick crosses (also presented in Figs. 5-7). Literature data (Supplementary Table 3) for the CLP loess and paleosol and global loess are also plotted for comparison (also in Figs. 5&6). The symbols are the same in the following Figs. 5-7.

Fig. 5 (a-l) Correlation diagrams of representative analyzed elements (HFSEs-transition metals-Ga-Sn) with La. (m-n) Correlation diagrams of Nb-Ta and Zr-Hf. (o-p) Co-variation diagrams between Th/Pb vs. U/Pb, and Mo and U for loess and paleosol samples from the CLP. The correlation coefficients in (a, b, d, e, g, k) also include the data on the CLP loess by Chauvel et al. (2014).

Fig. 6 Correlation diagrams of alkali and alkaline earth elements with La (a-f) and their correlations with micas + clay minerals + K-feldspar, which are thought to the important mineral hosts for these elements (g-h) for loess and paleosol samples from the CLP. The correlation coefficients are given for analytical data of the CLP loess samples of this study and updated data on the CLP loess by Chauvel et al. (2014), except Be, contents of which are not available in the latter.

Fig. 7 Correlation diagrams of Rb/Sr and $^{87}Sr/^{86}Sr$ ratios with CaO, Sr, Rb and mineral modal abundances to illustrate the influence of carbonate on these geochemical variations. More carbonate leads to increasing Sr content, while the decrease of micas + clay minerals + K-feldspar can lead to decreasing Rb content, both of which will result in the decrease of Rb/Sr and $^{87}Sr/^{86}Sr$ ratios finally.

Fig. 8 The recommended values of the UCC composition in this study normalized to those recommended by Rudnick and Gao (2003). Major elements are in wt.% (a), while trace elements are in ppm (b). The lighter grey area represents the agreement of the recommended values within ± 20%. The recommended values of Taylor and McLennan (1985) with updates by McLennan (2001), Gao et al. (1998; carbonate-bearing composition), and Gaschnig et al. (2016) are also given for comparison.

Fig. 9 (a) The modelling diagram to show the difference between peridesert loess and periglacial loess. Although chemical alteration during the processes to produce loess is limited, Ba – Rb – Cs – K as fluid-soluble elements lack correlation with La in previously studied loess, which likely reflect the heterogeneous composition of source rocks after an ineffective mixing. Hence, the observed correlation of Ba – Rb – Cs – K with La in Fig. 6 of this study indicates that dust materials for the CLP loess has experienced effective mixing after a long-distance transport. (b) The comparison of Ba – Cs contents of this study with previous estimates, i.e., G98 - Gao et al., 1998 (including both carbonate-bearing and carbonate excluded, the plot with slash); G16 – Gaschnig et al., 2016; W95 - Wedepohl, 1995; RG03 - Rudnick and Gao, 2003; TM85 - Taylor and McLennan, 1985 (related data are given in Table 1).

Table 1: Recommended values of the UCC composition in different estimates (major elements are in wt.%, and trace elements are in ppm).

Supplementary Materials

Supplementary Table 1: Analyzed results of loess and paleosol samples from the Chinese Loess Plateau in this study (major elements are in wt.%, and trace elements are in ppm).

Supplementary Table 2: Strontium isotope composition of loess and paleosol samples from the CLP.

Supplementary Table 3: Compiled geochemical data for global loess and paleosol samples in the literature (major elements in wt.%, trace elements in ppm).

Supplementary File A: Data quality of major and trace element analyses.

Supplementary File B: Petrographic studies, presenting correlations of major element contents with mineral modal abundances using data in literature and photomicrographs.

Xiao et al., Fig.1 Distributions of global loess

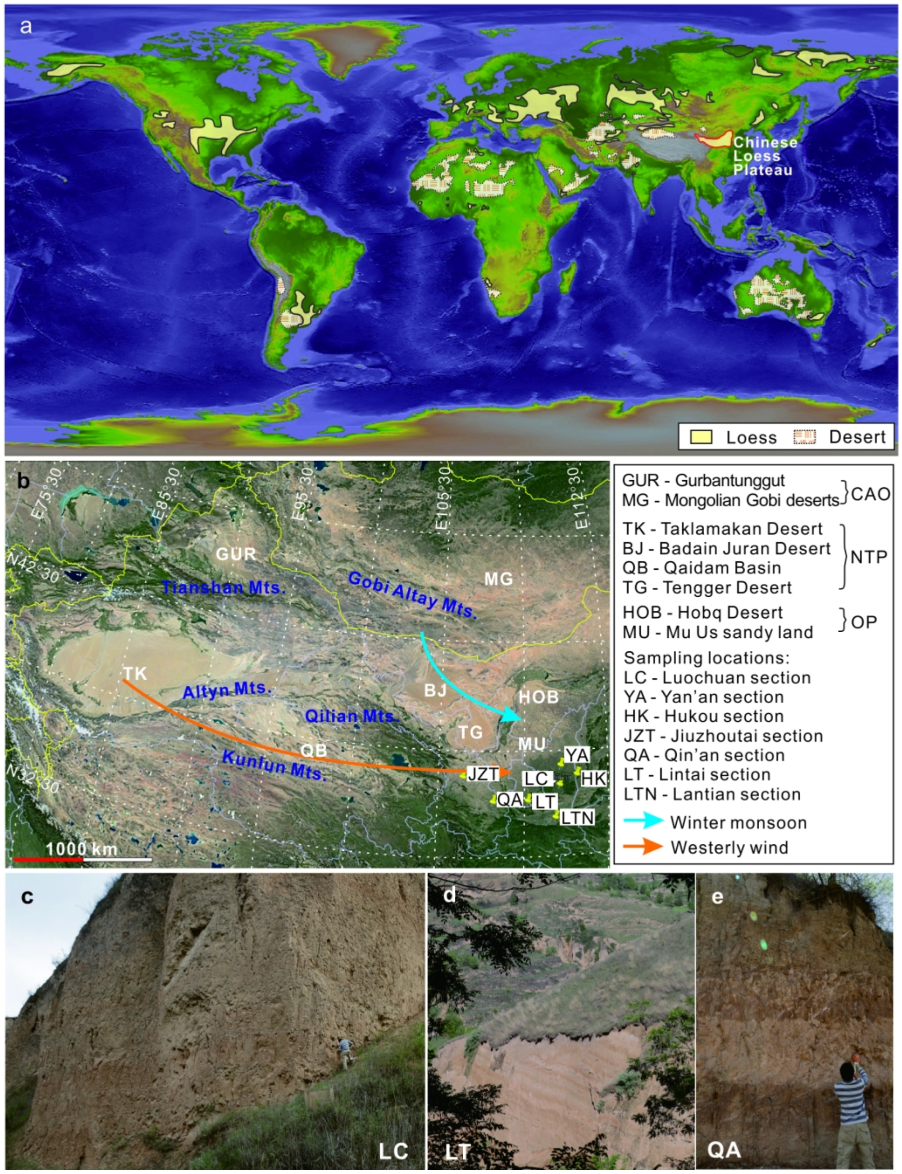

Fig. 1 Distributions of global loess and sampling locations

146x195mm (300 x 300 DPI)

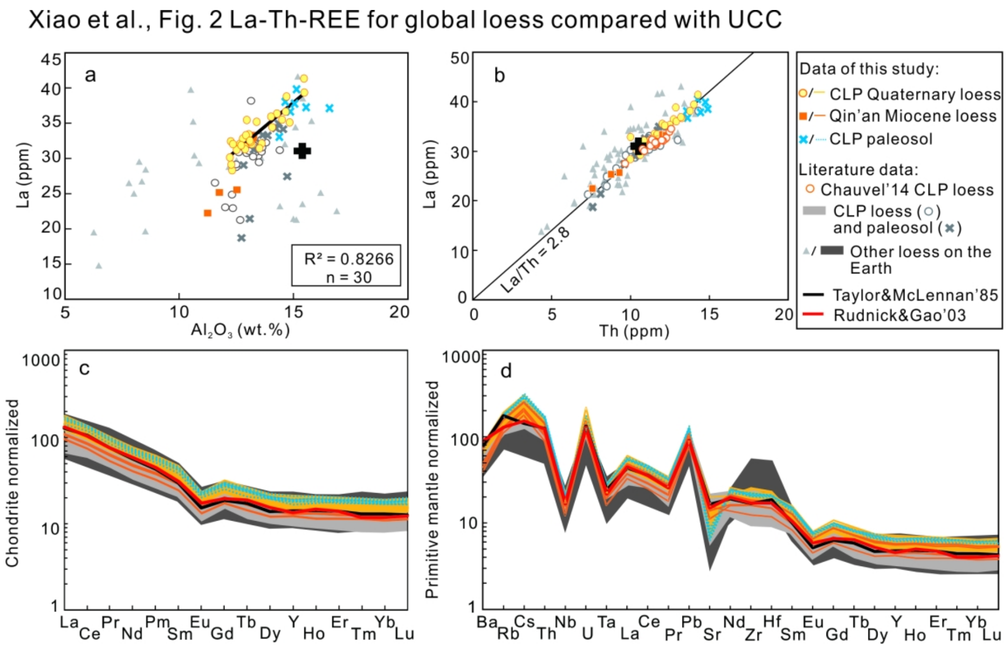

Figure 2 La-Th for global loess compared with UCC

175x111mm (300 x 300 DPI)

Xiao et al., Fig. 3 Photomicrographic images and counting results by SEM-EDS

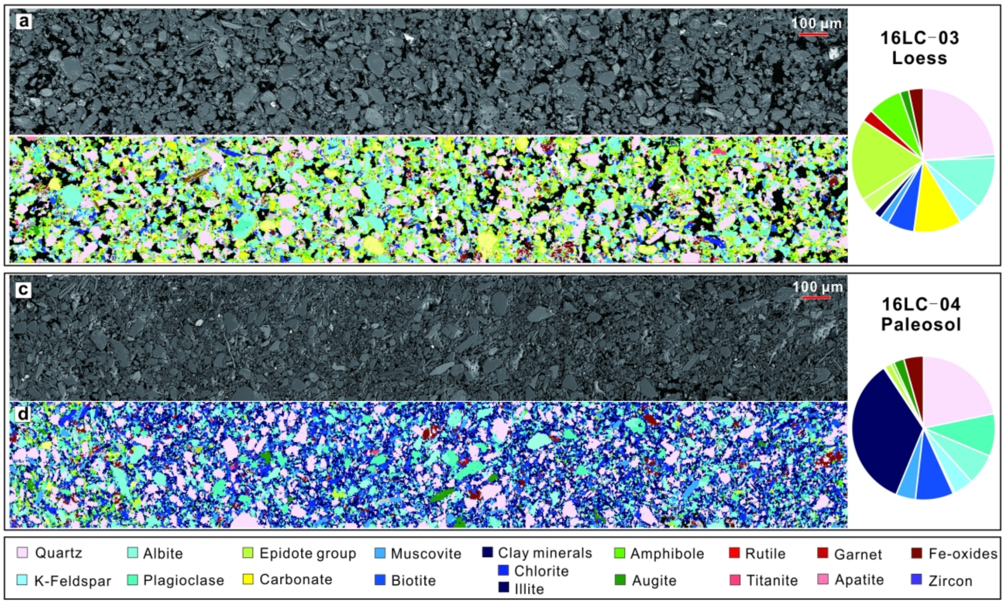

Fig. 3 Photomicrographic images

198x125mm (300 x 300 DPI)

Xiao et al., Fig.4 Co-variations of major elements

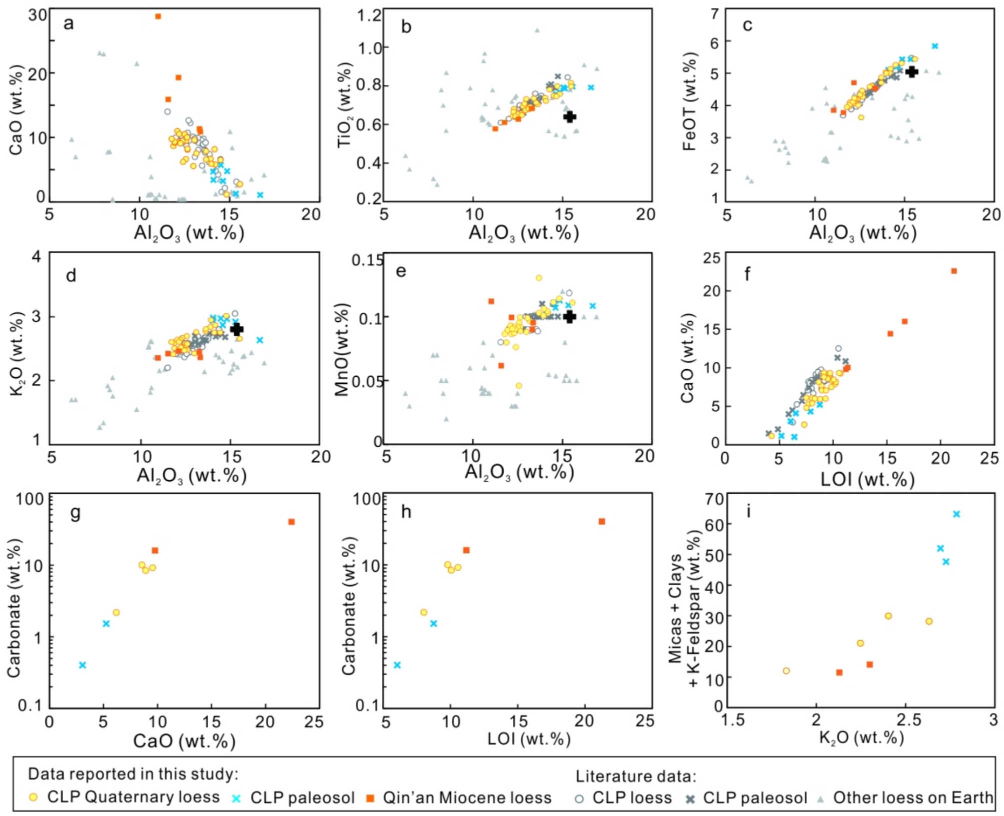

Figure 4 Co-variation diagrams of major elements

174x150mm (300 x 300 DPI)

Xiao et al., Fig. 5 Co-variations of transition metals

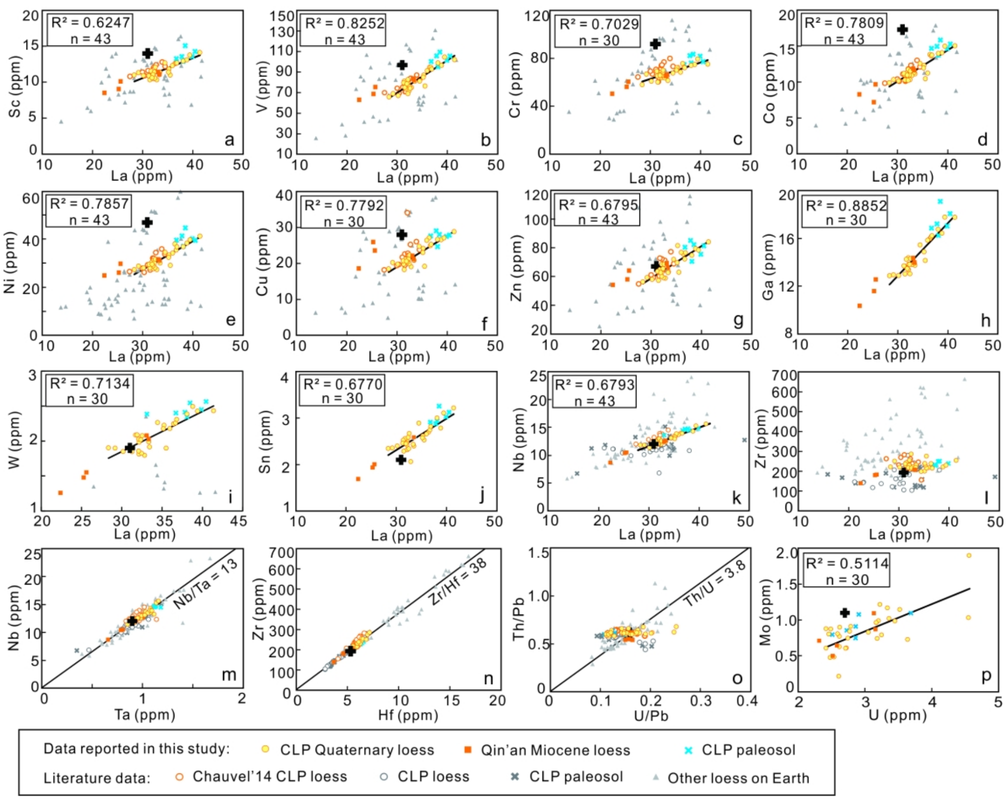

Figure 5 Co-variation diagrams of HFSE-transition metals-Th-U

197x162mm (300 x 300 DPI)

Xiao et al., Fig. 6 Co-variations of alkali and alkaline elements

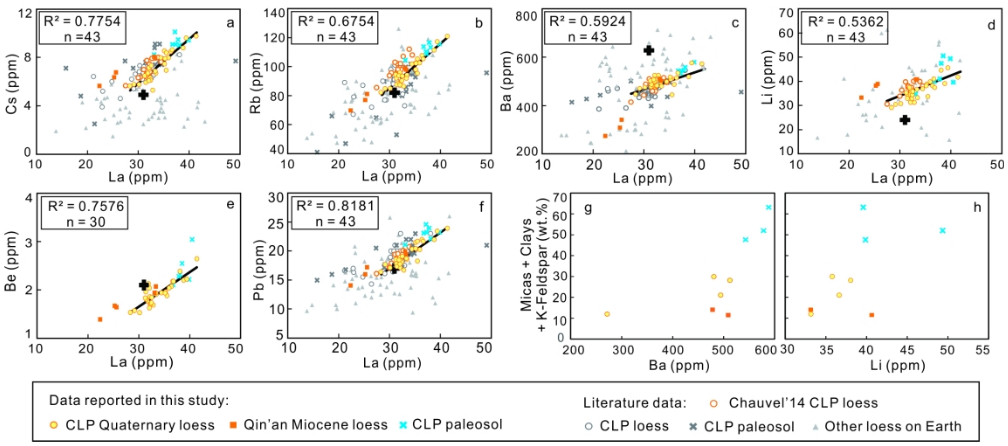

Figure 6 Co-variation diagrams of alkali

204x97mm (300 x 300 DPI)

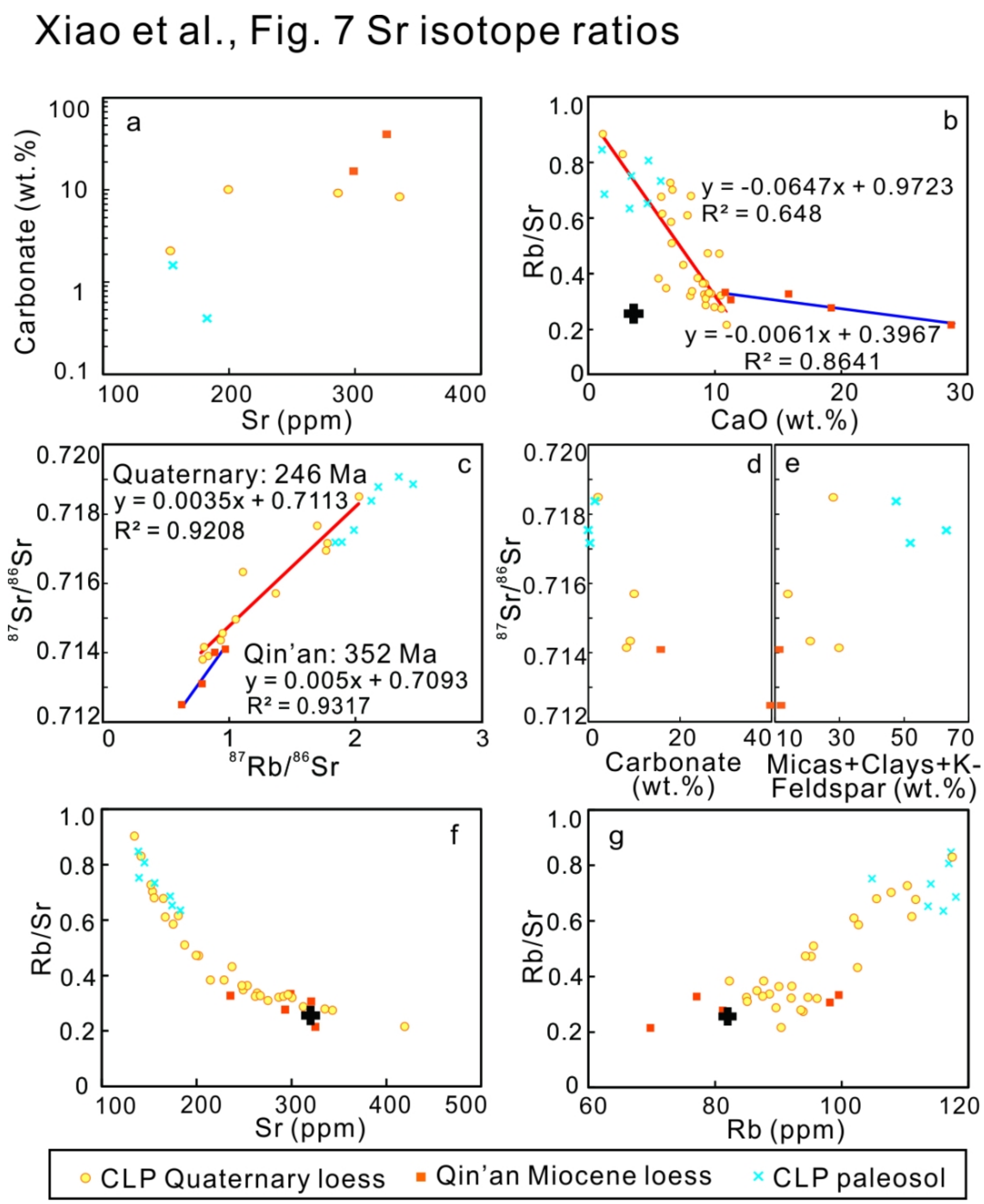

Figure 7 Sr isochron

103x126mm (300 x 300 DPI)

Xiao et al., Fig. 8 Comparison with recommended values of UCC

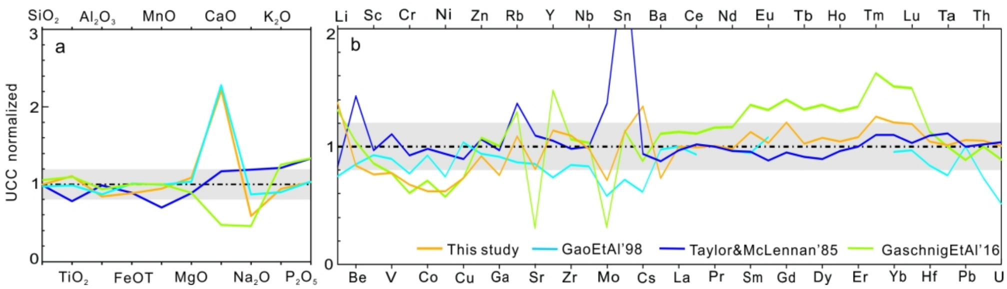

Figure 8 Comparison with recommended values of UCC

195x63mm (300 x 300 DPI)

Xiao et al., Fig. 9 Model diagram

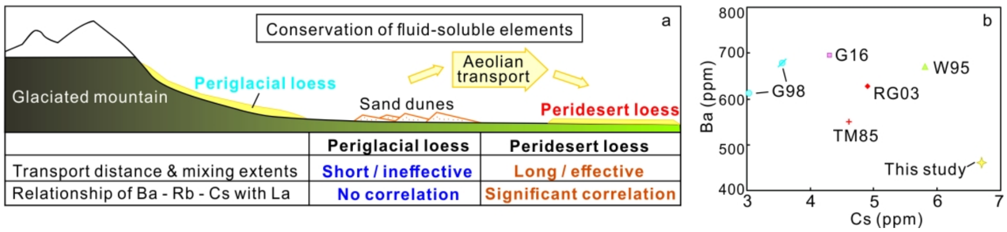

Fig. 9 Modal diagram

171x50mm (300 x 300 DPI)

Table 1: Recommended values of the UCC composition in different estimates (major elements are in wt.%, and trace elements are in ppm).

No.	1	2	3	4	5		6	7		8		9		10		11	
Ref.	Shaw et al., 1967, 1976	Wedepohl, 1995[a]	Fahrig and Eade, 1968; Eade & Fahrig, 1973	Condie, 1993	Gao et al., 1998	Gao et al., 1998	Taylor and McLennan, 1985, 1995; McLennan, 2001	Rudnick and Gao, 2003		Hu & Gao, 2008		Gaschnig et al., 2016		Others		This study[b]	
					Carbonate-free based	Carbonate-bearing		Value	1 sigma	Value	1 sigma	No carbonate-rich diamictite	All samples	Value	Ref.	Value	1 sigma
SiO_2	66.8		66.2	67	67.97	64.56	65.89	66.6	1.18			70.4	70.2			66.37	1.84
TiO_2	0.54		0.54	0.56	0.67	0.63	0.50	0.64	0.08			0.70	0.70			0.71	0.05
Al_2O_3	15.05		16.1	15.14	14.17	13.39	15.17	15.4	0.75			14.6	14.4			12.98	0.97
FeOT	4.09		4.4	4.76	5.33	5.08	4.49	5.04	0.53			4.95	5.04			4.46	0.47
MnO	0.07		0.08		0.1	0.10	0.07	0.10	0.01			0.10	0.10			0.09	0.01
MgO	2.3		2.2	2.45	2.62	2.56	2.2	2.48	0.35			2.00	2.20			2.70	0.39
CaO	4.24		3.4	3.64	3.44	8.18	4.19	3.59	0.2			1.40	1.70			7.96	2.31
Na_2O	3.56		3.9	3.55	2.86	2.84	3.89	3.27	0.48			1.60	1.50			1.94	0.29
K_2O	3.19		2.91	2.76	2.68	2.51	3.39	2.80	0.23			3.60	3.50			2.64	0.18
P_2O_5	0.15		0.16	0.12	0.16	0.15	0.20	0.15	0.02			0.20	0.20			0.15	0.02
Li	22				20	18	20	24	5	41	6	31.3	31.4	35 ± 11	Teng et al., 2004	34	5
Be	1.3	3.1			1.95	1.78	3	2.1	0.9	1.9	0.2	2.34	2.19			1.8	0.3
Sc	7		12	13.4	15	13	13.6	14	0.9	14	1	12.1	12			11[c]	1
V	53		59	86	98	87	107	97	11	106	7	73.8	75			75	11
Cr	35		76	112	80	71	85	92	17	73	10	53	55.7			64	7
Co	12			18	17	16	17	17.3	0.6	15	1	11.8	12.3			11	2
Ni	19		19	60	38	35	44	47	11	34	5	26.3	27			29	4
Cu	14		26		32	29	25	28	4	27	2	20.2	20.5			21	4
Zn	52		60		70	63	71	67	6	75	9	73	72			63	9
Ga	14				18	16	17	17.5	0.7	18.6	0.8	18.2	17.6			14	2
Rb	110	110	85	83	82	71	112	82	17	94	7	110	106			92	12
Sr	316		380	289	266	273	350	320	46			91.5	99.1			259[d]	80
Y	21		21	24	17.4	15.5	22	21	2			33.2	31			25	3
Zr	237		190	160	188	163	190	193	28			220	205			217	29

Table 1 Continued.

	1	2	3	4	5		6	7		8		9		10		11	
Nb	26			9.8	12	10	12	12	1	11.6	0.5	12.7	12.4	13.7	Plank & Langmuir, 1998	12.1	1.4
Mo		1.4			0.78	0.64	1.5	1.1	0.3	0.6	0.3	0.3	0.35	1.2	Sims et al., 1990	0.8[d]	0.3
Sn		2.5			1.73	1.51	5.5	2.1	0.5	2.2	0.2	2.41	2.38			2.4	0.3
Cs		5.8			3.55	3.02	4.6	4.9	1.5	4.9	0.3	4.3	4.3	7.3	Plank & Langmuir, 1998	**6.7**	1.2
Ba	1070	668	730	633	678	613	550	628	83			731	696			**461**	51
La	32.3		71	28.4	34.8	31	30	31	3			36.5	34.9			31[e]	4
Ce	65.6			57.5	66.4	58.7	64	63	4			72.9	70			63	8
Pr		6.3					7.1	7.1				8.54	8.25			7.2	0.9
Nd	25.9			25.6	30.4	26.1	26	27	2			33.3	31.5			27	3
Sm	4.61	4.7		4.59	5.09	4.45	4.5	4.7	0.3			6.84	6.36			5.3	0.6
Eu	0.937	0.95		1.05	1.21	1.08	0.88	1	0.1			1.37	1.31			1.03	0.12
Gd		2.8		4.21			3.8	4	0.3			6.05	5.6			4.8	0.6
Tb	0.481			0.66	0.82	0.69	0.64	0.7	0.1			0.983	0.92			0.73	0.09
Dy	2.9						3.5	3.9				5.57	5.28			4.2	0.5
Ho	0.62						0.8	0.83				1.13	1.08			0.87	0.10
Er							2.3	2.3		2.30		3.27	3.08			2.5	0.3
Tm							0.33	0.3		0.37	0.01	0.506	0.487			0.38	0.05
Yb	1.47			1.91	2.26	1.91	2.2	2	0.4	2.34	0.03	3.07	3.02			2.4	0.3
Lu	0.233			0.32	0.35	0.3	0.32	0.31	0.05	0.36	0.01	0.479	0.464			0.37	0.05
Hf	5.8		4.3	5.12		4.45	5.8	5.3	0.7			6.5	5.98			5.5	0.7
Ta	5.7	1.5		0.79	0.74	0.68	1	0.9	0.1	0.92	0.03	0.94	0.901	0.96	Plank & Langmuir, 1998	0.92	0.11
Pb		17	18	17	18	17	17	17	0.5			15.8	15.1			18	2
Th	10.3		10.8	8.6	8.95	7.71	10.7	10.5	1			11.3	10.5			11.0	1.4
U	2.45		1.5	2.2	1.55	1.39	2.8	2.7	0.6	2.6	0.1	2.66	2.4			2.7[d]	0.5

a: Updates of Shaw et al., 1967, 1976. **b:** Values of major elements are the average composition of the CLP Quaternary loess samples recalculated to a major-element sum of 100% in this study. Considering the significant correlations of most analyzed elements with La, values of trace elements in the UCC are calculated by using the average La/X ratios (X is contents of the element of interest) and the widely accepted La content of 31 ppm. **c:** The values in red are the suggested updates of the UCC composition in this study. **d:** As Sr negatively correlates with La, we use the correlation of Sr with 1/La to estimate the Sr value of the UCC by assuming La of 31 ppm. Values of Mo and U are their average contents in the CLP loess samples, which are presented only for reference considering their differentiation from other elements during the sedimentary processses to produce the CLP loess. **e:** The recommended value is refered to Rudnick and Gao (2003).

Supplementary File A Data quality of major and trace element analysis as well as iron isotope composition.

Table DR1. Major element analysis of international standards

	BHVO-2						AGV-2			GSP-2				
	Rec. (wt.%)	Meas. (wt.%)		AVG (wt.)	RSD (%)	RE (%)	Rec. (wt.%)	Meas. (wt.%)	RE (%)	Ref. (wt.%)	Meas. (wt.%)		AVG (wt.)	RSD (%)
SiO_2	49.60	50.78	50.64	50.71	0.2	2.2	59.14	60.09	1.6	62.7 - 67.7	68.66	67.11	67.88	1.6
TiO_2	2.73	2.76	2.77	2.76	0.2	1.2	1.05	1.04	-1.5	0.59 - 0.92	0.68	0.66	0.67	1.9
Al_2O_3	13.44	13.16	13.19	13.18	0.1	-2.0	17.03	16.39	-3.7	14.59 - 21.5	14.62	14.23	14.43	1.9
Fe_2O_3T	12.39	12.15	12.16	12.15	0.1	-1.9	6.78	6.65	-2.0	4.08 - 4.96	4.96	4.85	4.91	1.5
MnO	0.17	0.17	0.17	0.17	0.01	0.1	0.10	0.10	-0.8	0.038 - 0.06	0.0424	0.0419	0.042	0.8
MgO	7.26	7.31	7.32	7.32	0.05	0.8	1.80	1.82	0.9	0.91 - 1.3	0.99	0.97	0.98	1.3
CaO	11.40	11.33	11.39	11.36	0.3	-0.3	5.15	5.20	1.0	2.02 - 2.84	2.16	2.17	2.17	0.6
Na_2O	2.22	2.23	2.21	2.22	0.6	0.1	4.02	4.22	5.0	1.02 - 3.62	2.86	2.84	2.85	0.5
K_2O	0.51	0.53	0.51	0.52	2.3	1.0	2.90	2.93	1.2	2.89 - 5.67	5.54	5.50	5.52	0.4
P_2O_5	0.27	0.27	0.27	0.27	1.5	0.5	0.48	0.48	-0.9	0.24 - 0.33	0.30	0.30	0.30	0.2

Meas.: Measured values. Rec.: recommended values. AVG: average. RE: relative error between measured and recommended values. RSD: relative standard deviation. Recommended values and reference values are from http://georem.mpch-mainz.gwdg.de/sample_query_pref.asp.

Table DR2. Replicate analysis of major elements

	16HK-03A			16HK-05B		
	16HK-03A (wt.%)	16HK-03A (wt.%)	RSD (%)	16HK-05B (wt.%)	16HK-05B (wt.%)	RSD (%)
SiO_2	61.47	62.12	0.7	60.30	61.13	1.0
TiO_2	0.65	0.65	0.4	0.62	0.62	0.2
Al_2O_3	11.73	11.83	0.6	11.20	11.25	0.3
Fe_2O_3T	4.49	4.52	0.5	4.20	4.22	0.4
MnO	0.09	0.09	2.9	0.08	0.08	0.09
MgO	2.59	2.61	0.6	2.40	2.41	0.4
CaO	7.49	7.41	0.8	8.39	8.30	0.8
Na_2O	2.03	2.05	0.7	1.74	1.74	0.2
K_2O	2.38	2.42	1.1	2.28	2.31	0.9
P_2O_5	0.15	0.15	0.4	0.14	0.13	3.0

Table DR3. Trace element analysis of international standards

	Iso.	BCR-2 Meas.	BCR-2 Jochum et al., 2016 Rec.	BCR-2 Jochum et al., 2016 Uncertainty	BCR-2 RE (%)	AGV-2 Meas.	AGV-2 Jochum et al., 2016 Rec	AGV-2 Jochum et al., 2016 Uncertainty	AGV-2 RE (%)	GSP-2 Meas.	GSP-2 Ref.
Li	7	8.76	9.13	0.22	-4.0	10.48	10.8	0.21	-3.0	36.12	31.1 - 51
Be	9	2.33	2.17	0.1	7.5	2.11	2.209	0.066	-4.4	1.49	0.92 - 1.92
Sc	45	32.15	33.53	0.4	-4.1	12.22	13.11	0.31	-6.8	6.56	5 - 8.32
V	51	435	417.6	4.5	4.1	122	118.5	1.2	2.9	54.03	42 - 59
Cr	53	14.19	15.85	0.38	-10	15.20	16.22	0.72	-6.3	18.27	15.6 - 62.9
Co	59	36.55	37.33	0.37	-2.1	15.15	15.46	0.5	-2.0	6.98	3.72 - 7.6
Ni	60	11.06	12.57	0.3	-12	17.39	18.87	0.41	-7.9	14.83	1.99 - 21
Cu	63	17.29	19.66	0.72	-12	49.11	51.51	0.65	-4.6	38.75	22.6 - 47
Zn	66	133	129.5	1.8	3.1	90.67	86.7	1.2	4.6	120	75 - 137.13
Ga	71	21.14	22.07	0.19	-4.2	19.60	20.42	0.17	-4.0	22.84	19.6 - 29.71
Rb	85	45.71	46.02	0.56	-0.7	65.85	67.79	0.66	-2.9	239	193 - 274
Sr	88	344	337.4	6.7	1.8	668	659.5	5.7	1.3	242	209 - 259
Y	89	33.61	36.07	0.37	-6.8	18.44	19.14	0.84	-3.7	25.49	22 - 30
Zr	90	181.9	186.5	1.5	-2.5	230	232	2.3	-1.0	550	139 - 642
Nb	93	11.92	12.44	0.2	-4.2	13.61	14.12	0.22	-3.6	26.52	18 - 30.9
Mo	95	248	250.6	6.7	-0.9	1.87	2	0.11	-6.4	2.21	1.34 - 4
Sn	118	1.94	2.28	0.13	-15	1.82	1.83	0.25	-0.4	6.54	1.184-8.32
Cs	133	1.13	1.16	0.023	-2.5	1.16	1.173	0.018	-1.0	1.19	0.98 - 1.4
Ba	137	694	683.9	4.7	1.5	1172	1134	8	3.4	1411	1149 - 1491
La	139	24.87	25.08	0.16	-0.9	38.18	38.21	0.38	-0.08	192	159 - 205
Ce	140	52.50	53.12	0.33	-1.2	69.77	69.43	0.57	0.5	457	343.9 - 498
Pr	141	6.56	6.83	0.044	-3.9	8.07	8.165	0.084	-1.1	58.23	47.1 - 61.3
Nd	146	27.84	28.26	0.37	-1.5	29.87	30.49	0.47	-2.0	213	177.8 - 247
Sm	147	6.37	6.55	0.047	-2.7	5.43	5.509	0.078	-1.4	26.01	23.1 - 29.3
Eu	151	1.91	1.99	0.024	-3.8	1.54	1.553	0.015	-1.0	2.24	1.96 - 2.61
Gd	156	6.69	6.81	0.078	-1.8	4.43	4.678	0.064	-5.3	12.87	10.1 - 14.9
Tb	159	1.02	1.08	0.026	-5.0	0.63	0.651	0.0073	-3.6	1.31	1.09-1.54
Dy	163	6.04	6.42	0.055	-5.9	3.32	3.549	0.031	-6.4	5.50	5.08 - 6.63
Ho	165	1.26	1.31	0.011	-3.8	0.66	0.68	0.0081	-2.7	0.95	0.8 - 1.09
Er	167	3.50	3.67	0.038	-4.6	1.78	1.825	0.013	-2.6	2.25	2.02 - 2.77
Tm	169	0.52	0.53	0.006	-2.9	0.26	0.2623	0.0035	-1.9	0.30	0.23 - 0.32
Yb	173	3.28	3.39	0.036	-3.4	1.55	1.653	0.013	-6.2	1.62	1.23 - 1.85
Lu	175	0.49	0.50	0.0078	-2.5	0.25	0.2507	0.0033	0.02	0.23	0.16 - 0.26
Hf	178	4.81	4.97	0.034	-3.2	5.08	5.137	0.057	-1.0	13.71	1.81 - 16.7
Ta	181	0.81	0.78	0.018	2.7	0.87	0.865	0.019	0.04	0.88	0.43 - 1.01
W	182	0.47	0.46	0.05	1.2	0.50	0.553	0.094	-9.9	0.35	0.29 - 0.39
Pb	208	9.66	10.59	0.17	-8.8	12.70	13.14	0.15	-3.3	41.65	35.385 -
Th	232	5.81	5.83	0.05	-0.3	6.14	6.174	0.063	-0.6	113	92 - 122
U	238	1.64	1.68	0.017	-2.5	1.88	1.885	0.015	-0.1	2.49	1.8 - 3

Meas.: Measured values in ppm. Iso.: isotope. Rec.: recommended values in ppm. Ref.: reference values in ppm. RE: relative error between measured and recommended values. RSD: relative standard deviation. Recommended values and reference values are from http://georem.mpch-mainz.gwdg.de/sample_query_pref.asp.

Table DR4. Replicate analysis of trace elements

	16LTN-02a			16QA-04a			16LC-06a			JZT16-05a		
	200528A 41.d	200528 A51.d	RSD (%)	200528 A34.d	200528 A55.d	RSD (%)	200528 A19.d	200528 A54.d	RSD (%)	200528 A26.d	200528 A53.d	RSD (%)
Li	40.93	42.81	3.2	40.72	42.76	3.5	40.98	42.08	1.9	34.38	34.27	0.2
Be	2.17	2.28	3.3	2.07	2.01	1. 9	2.28	2.32	1.4	1.73	1.86	5.0
Sc	12.64	12.49	0.8	11.10	11.23	0.8	13.59	13.52	0.4	10.58	10.39	1.3
V	94.66	95.40	0.5	82.01	83.01	0.9	105.8	107.0	0.8	75.58	76.70	1.0
Cr	72.56	72.86	0.3	66.41	66.80	0.4	82.19	79.99	1.9	68.17	68.86	0.7
Co	13.61	13.68	0.4	11.63	11.99	2.1	14.95	15.27	1.5	10.31	10.49	1.2
Ni	35.57	35.38	0.4	31.35	31.83	1.	41.47	41.91	0.7	28.14	28.51	0.9
Cu	24.98	24.98	0.0	21.22	21.40	0.6	29.11	29.51	1.1	19.96	20.11	0.5
Zn	72.20	71.86	0.3	66.33	65.53	0.9	85.09	81.67	2.9	59.05	60.43	1.6
Ga	16.09	16.07	0.1	13.96	14.28	1.6	17.18	17.32	0.5	13.02	13.19	0.9
Rb	105.6	104.9	0.4	98.16	100.8	1.9	116.9	118.0	0.6	90.51	91.03	0.4
Sr	155.3	154.4	0.4	320.8	326.2	1.2	144.8	146.6	0.8	419.5	430.1	1.7
Y	27.24	26.99	0.7	25.40	26.30	2.5	28.16	28.26	0.3	27.17	25.13	5.5
Zr	214.2	203.5	3.6	205.4	214.7	3.1	248.4	233.3	4.4	285.7	256.7	7. 6
Nb	13.90	13.70	1.0	12.60	12.80	1.1	14.77	16.78	9.0	11.91	11.94	0.1
Mo	0.87	0.84	2.6	0.87	0.90	2.1	0.91	0.93	1.2	1.03	1.11	5.1
Sn	2.75	2.77	0.4	2.56	2.59	0.7	2.98	2.89	2.4	2.36	2.35	0.5
Cs	8.62	8.63	0.03	7.91	8.05	1.3	9.47	9.57	0.8	6.11	6.26	1.7
Ba	533.5	529.9	0.5	501.0	508.0	1.0	545.5	550.8	0.7	503.1	505.6	0.3
La	36.67	36.54	0.2	33.34	32.02	2.9	37.82	36.89	1.7	32.46	31.94	1.1
Ce	73.71	73.72	0.02	67.15	64.42	2.9	81.68	79.41	2.0	66.00	64.54	1.6
Pr	8.41	8.38	0.3	7.64	7.33	3.0	8.82	8.63	1.5	7.60	7.34	2.4
Nd	30.89	30.35	1.2	28.76	27.61	2.9	32.32	31.71	1.3	28.21	26.86	3.5
Sm	6.14	6.13	0.2	5.64	5.54	1.3	6.37	6.35	0.2	5.65	5.33	4.1
Eu	1.18	1.17	0.8	1.10	1.06	2. 9	1.26	1.25	0.7	1.06	1.07	0.5
Gd	5.58	5.58	0.03	5.20	5.23	0.4	5.53	5.72	2.5	5.31	5.04	3.7
Tb	0.83	0.84	1.0	0.78	0.79	1.6	0.87	0.87	0.6	0.79	0.75	3.3
Dy	4.66	4.75	1.3	4.40	4.54	2.2	4.97	5.05	1.0	4.57	4.24	5.2
Ho	0.99	0.97	1.5	0.93	0.96	2.0	1.04	1.04	0.1	0.96	0.89	5.3
Er	2.77	2.77	0.07	2.59	2.70	2.9	2.97	2.89	2.0	2.82	2.53	7.4
Tm	0.42	0.43	0.07	0.40	0.42	3.4	0.46	0.46	0.5	0.46	0.40	9.2
Yb	2.69	2.67	0.5	2.54	2.60	1.7	2.98	2.85	3.0	2.97	2.51	11.9
Lu	0.42	0.43	1.0	0.39	0.41	2.7	0.46	0.44	2.5	0.47	0.39	12.2
Hf	5.56	5.37	2.4	5.29	5.58	3.8	6.51	6.15	4.0	7.15	6.61	5.5
Ta	1.08	1.07	0.8	1.01	1.03	1.5	1.14	1.29	8.8	0.92	0.93	0.9
W	2.26	2.26	0.1	2.02	2.03	0.1	2.41	2.46	1.3	1.82	1.82	0.2
Pb	21.68	21.53	0.5	19.42	19.62	0.7	23.95	24.09	0.4	18.09	18.11	0.08
Th	13.27	13.14	0.7	12.02	12.05	0.2	14.44	14.17	1.3	12.26	12.11	0.8
U	2.49	2.49	0.01	3.16	3.18	0.6	2.86	2.76	2.5	4.55	4.39	2.5

Supplementary File B Petrographic studies, presenting co-variations of major element contents with mineral modal abundances using data in literature and photomicrographs of our samples.

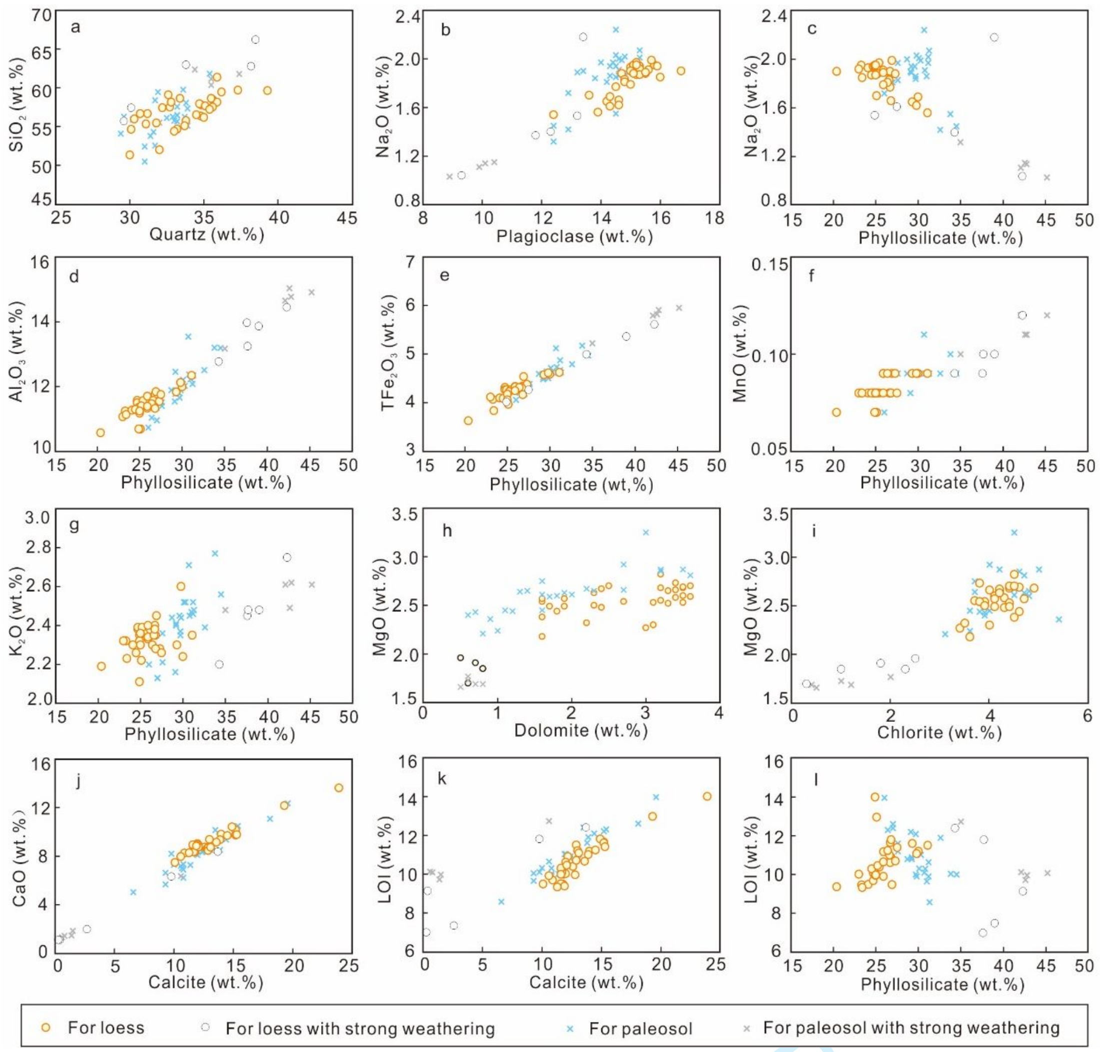

Figure A. Co-variation diagrams of bulk-rock major element contents with mineral modal abundances for the CLP loess and paleosol (all these compiled data are referred to Jeong et al., 2008, 2010, whose data are systematic). (a) SiO_2 is significantly correlated with quartz. (b-c) Na_2O positively correlates with plagioclase while negatively correlates with phyllosilicate. (d-g) Al_2O_3 – TFe_2O_3 – MnO – K_2O are correlated with phyllosilicate (i.e., micas, kaolinite, chlorite, and other clay minerals such as illite, smectite, vermiculite). (h-i) Co-variations of MgO with minerals, reflecting its correlation with chlorite. (j) CaO is strictly correlated with calcite, and (k-l) LOI correlates with both calcite and phyllosilicate minerals.

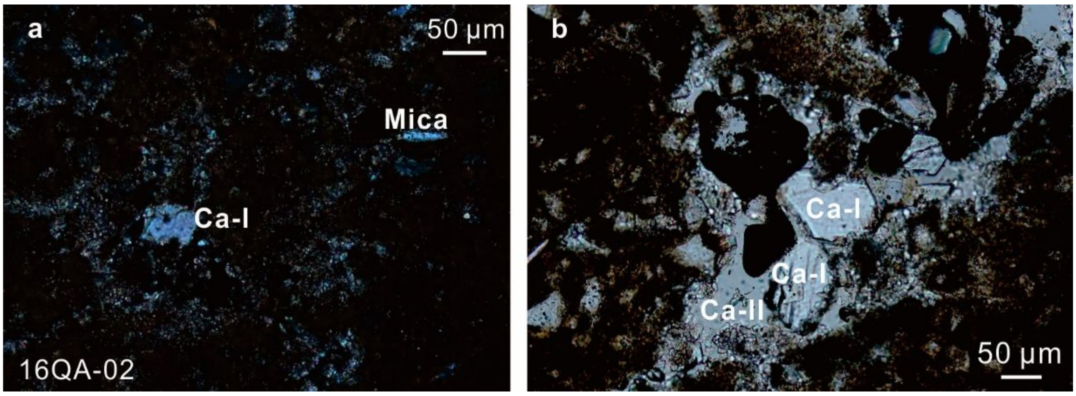

Figure B. Representative petromicrographs of the CLP loess samples, showing the common presence of carbonate.

References:

Jeong, G.Y., Hillier, S., Kemp, R.A., 2008. Quantitative bulk and single-particle mineralogy of a thick Chinese loess–paleosol section: implications for loess provenance and weathering. Quaternary Science Reviews 27, 1271-1287.

Jeong, G.Y., Hillier, S., Kemp, R.A., 2011. Changes in mineralogy of loess–paleosol sections across the Chinese Loess Plateau. Quaternary Research 75, 245-255.

Supplementary Table 1: Analyzed results of loess and paleosol samples from the Chinese Loess Plateau in this study (major elements are in wt.%, and trace elements are in ppm)

		Qin'an Loess					Luochuan Loess						Luochuan Paleosol						
Location		34°56'21"N, 105°33'7"E		35°2'24"N, 105°26'59"E	34°59'N, 105°32'E		35°42'N, 109°25'E											36°9'N, 110°26'E	
Sample		16QA-01a	16QA-02a	16QA-03A	16QA-04a	16QA-05a	16LC-01a	16LC-03a	16LC-05	16LC-07	16LC-09a	16LC-10a	16LC-02a	16LC-04a	16LC-06a	16LC-08a	16LC-11a	16HK-01a	16HK-02a
SiO2		47.60	38.52	53.32	55.64	57.16	58.39	59.68	62.72	62.06	64.59	62.44	62.72	64.92	62.90	61.42	65.75	59.44	64.63
TiO2		0.53	0.46	0.54	0.61	0.62	0.62	0.62	0.72	0.71	0.69	0.70	0.71	0.75	0.76	0.71	0.73	0.59	0.62
Al2O3		10.14	8.60	9.99	11.84	12.08	11.28	11.40	13.29	12.96	11.66	12.72	12.97	13.76	13.87	13.34	13.28	10.94	11.57
TFe2O3		3.91	3.33	3.61	4.46	4.55	4.33	4.31	5.33	5.19	3.73	4.85	5.11	5.46	5.63	5.30	5.34	4.05	4.14
MnO		0.08	0.09	0.05	0.080	0.086	0.08	0.09	0.10	0.09	0.04	0.12	0.10	0.10	0.11	0.10	0.10	0.08	0.07
MgO		2.19	1.99	1.90	2.66	2.55	2.22	2.15	2.43	2.31	2.06	2.43	2.14	2.19	2.32	2.38	2.20	2.60	2.37
CaO		16.04	22.40	13.67	10.02	9.80	9.34	8.57	5.41	6.21	6.14	6.08	4.32	3.07	4.44	5.27	3.20	8.35	5.76
Na2O		1.02	0.90	1.24	1.64	1.63	1.72	1.68	1.28	1.20	1.65	1.31	1.65	1.59	1.02	1.10	1.29	1.84	2.02
K2O		2.05	1.83	2.08	2.17	2.13	2.30	2.30	2.68	2.63	2.39	2.57	2.74	2.70	2.76	2.73	2.76	2.24	2.32
P2O5		0.15	0.17	0.14	0.12	0.15	0.13	0.13	0.12	0.13	0.12	0.16	0.12	0.10	0.11	0.12	0.10	0.14	0.13
LOI		16.68	21.27	15.33	11.38	11.20	10.71	9.82	7.72	8.04	8.31	9.31	6.53	6.06	7.89	8.77	6.62	9.87	7.52
TOTAL		100.40	99.57	101.88	100.61	101.95	101.13	100.73	101.80	101.52	101.36	102.69	99.10	100.70	101.80	101.24	100.79	100.13	101.16
Li	7	38.8	33.2	38.1	40.7	40.7	34.2	33.2	39.0	38.1	33.6	39.7	47.4	49.4	41.0	39.9	34.7	35.1	31.2
Be	9	1.64	1.39	1.67	2.07	1.93	1.85	1.91	2.20	2.07	1.88	2.04	2.32	2.21	2.28	2.10	1.90	1.72	1.69
Sc	45	10.1	8.52	9.07	11.1	11.4	11.0	11.4	13.1	12.6	11.0	12.3	12.9	13.6	13.6	13.3	12.8	10.5	10.3
V	51	75.3	62.9	68.6	82.0	83.6	79.3	80.9	96.5	94.5	76.3	91.3	95.1	101.5	105.8	100.3	89.1	76.2	75.0
Cr	53	60.4	50.4	56.2	66.4	65.2	63.7	61.4	74.8	75.6	72.2	68.4	76.2	81.8	82.2	74.8	69.0	65.6	63.6
Co	59	9.67	8.26	7.19	11.6	11.8	11.2	11.1	14.0	13.8	10.5	11.2	13.7	14.6	14.9	14.7	16.0	10.7	10.9
Ni	60	29.8	24.9	26.1	31.3	31.6	29.8	30.1	38.5	38.0	29.1	34.3	37.1	40.2	41.5	39.7	37.0	27.7	27.4
Cu	63	23.6	18.6	25.9	21.2	22.1	20.6	20.8	26.6	27.1	19.2	26.4	24.7	27.5	29.1	27.7	26.3	20.0	19.1
Zn	66	64.0	54.1	57.9	66.3	69.2	64.6	63.2	79.3	75.7	63.0	76.8	70.5	75.5	85.1	80.3	72.9	62.6	58.8
Ga	71	12.6	10.4	11.6	14.0	14.3	13.8	13.7	16.4	15.9	14.1	15.8	16.2	17.0	17.2	16.8	16.0	13.4	13.8
Rb	85	81.2	69.8	77.1	98.2	99.5	95.3	94.3	112	108	95.6	102.7	114	116	117	114	105	89.7	86.7
Sr	88	293	325	236	321	299	202	200	165	154	187	175	174	183	145	156	139	313	249
Y	89	20.6	19.1	20.2	25.4	26.3	24.8	25.6	31.3	27.9	27.5	26.3	29.5	29.6	28.2	27.9	25.9	24.8	22.8
Zr	90	182	139	179	205	207	220	231	221	238	275	217	250	238	248	227	241	255	222
Nb	93	10.5	8.7	10.4	12.6	12.4	12.5	12.5	14.3	14.0	13.5	13.7	14.5	14.8	14.8	14.4	13.6	12.0	12.3
Mo	95	0.65	0.71	0.50	0.87	1.09	0.63	0.75	0.77	0.81	0.22	0.48	0.75	1.08	0.91	0.86	0.88	0.74	0.48
Sn	118	2.01	1.69	1.94	2.59	2.58	2.51	2.40	2.79	2.70	2.53	2.66	2.95	3.03	2.89	2.92	2.83	2.32	2.07
Cs	133	6.76	5.63	6.35	7.91	8.04	7.01	6.68	8.78	8.48	6.93	7.96	9.02	9.43	9.47	9.08	8.24	6.20	5.29
Ba	137	339	272	306	501	509	476	478	517	512	442	485	556	578	546	543	492	490	523
La	139	25.6	22.4	25.3	33.3	33.1	32.2	33.5	38.8	36.4	35.5	36.0	38.1	39.9	37.8	36.7	33.1	32.1	32.8
Ce	140	51.8	44.8	50.5	67.1	66.0	64.6	67.4	74.4	73.8	72.1	74.7	76.9	81.9	81.7	77.6	71.4	64.2	66.3
Pr	141	5.94	4.98	5.77	7.64	7.46	7.43	7.70	8.69	8.39	8.18	8.46	8.74	9.16	8.82	8.61	7.84	7.35	7.56
Nd	146	22.2	18.7	21.5	28.8	28.4	27.1	27.8	31.8	30.9	30.0	30.8	32.0	33.5	32.3	31.1	29.5	27.0	27.8
Sm	147	4.41	3.70	4.34	5.64	5.63	5.44	5.63	6.35	6.05	5.99	6.14	6.43	6.76	6.37	6.27	5.80	5.40	5.47
Eu	151	0.91	0.76	0.86	1.10	1.11	1.06	1.10	1.25	1.18	1.15	1.19	1.24	1.29	1.26	1.22	1.16	1.07	1.08
Gd	156	4.10	3.52	4.13	5.20	5.25	5.00	5.08	5.94	5.47	5.47	5.45	5.76	5.93	5.53	5.57	5.13	4.85	4.67
Tb	159	0.62	0.53	0.61	0.78	0.79	0.75	0.78	0.91	0.84	0.83	0.83	0.87	0.90	0.87	0.87	0.76	0.75	0.69
Dy	163	3.51	3.05	3.50	4.40	4.55	4.24	4.48	5.25	4.81	4.74	4.70	5.10	5.21	4.97	4.90	4.88	4.24	4.02
Ho	165	0.73	0.64	0.74	0.93	0.96	0.90	0.94	1.09	0.99	0.98	0.98	1.09	1.08	1.04	1.02	0.98	0.89	0.83
Er	167	2.11	1.89	2.08	2.59	2.72	2.54	2.62	3.08	2.81	2.80	2.74	3.06	3.07	2.97	2.84	2.95	2.56	2.37
Tm	169	0.33	0.29	0.32	0.40	0.42	0.38	0.41	0.47	0.43	0.44	0.42	0.47	0.46	0.46	0.44	0.44	0.38	0.35

Yb	173	2.07	1.85	2.08	2.54	2.66	2.51	2.58	2.97	2.77	2.77	2.56	3.01	3.00	2.98	2.85	2.86	2.43	2.30
Lu	175	0.32	0.28	0.32	0.39	0.40	0.39	0.40	0.47	0.43	0.42	0.40	0.46	0.46	0.46	0.43	0.42	0.38	0.35
Hf	178	4.62	3.67	4.57	5.29	5.45	5.65	5.99	5.74	6.12	6.96	5.60	6.44	6.26	6.51	5.91	6.56	6.36	5.61
Ta	181	0.81	0.66	0.79	1.01	0.96	0.97	0.99	1.08	1.09	1.08	1.03	1.12	1.13	1.14	1.18	1.04	0.91	0.93
W	182	1.55	1.26	1.48	2.02	2.08	1.98	1.91	2.49	2.24	1.90	2.18	2.34	2.45	2.41	2.40	2.39	1.81	1.79
Pb	208	17.2	14.1	16.0	19.4	19.9	18.3	18.5	22.0	22.0	18.3	20.3	22.1	23.3	24.0	23.1	21.1	17.1	16.7
Th	232	9.31	7.59	8.76	12.0	12.2	11.2	11.5	12.9	12.7	12.0	12.9	13.6	14.7	14.4	13.6	12.3	11.5	10.0
U	238	2.58	2.32	2.52	3.16	3.13	2.62	2.74	2.62	2.59	2.61	2.48	2.86	2.91	2.86	2.73	2.63	3.18	2.54

	Yan'an-Hukou Loess					Lantian Loess			Lantian Paleosol		Lingtai Loess						
Location	36°10'N, 110°26'E		36°10'25"N, 110°25'50"E	36°37'22"N, 109°28'35"E	36°37'58"N, 109°24'28"E	34°10'N, 109°11'E					35°2'00"N, 107°31'6"E	34°58'N, 107°33'E					
Sample	16HK-03a	16HK-04a	16HK-05B	16YA-01a	16YA-02a	16LTN-01	16LTN-02a	16LTN-03	16LTN-04a	16LTN-05a	16LT-01a	16LT-02a	16LT-03a	16LT-04A	JZT16-01a	JZT16-02a	JZT16-03a
SiO2	61.47	60.22	60.30	65.05	62.52	61.37	58.95	65.05	67.11	65.34	59.07	68.43	62.55	59.46	60.69	58.85	58.68
TiO2	0.65	0.63	0.62	0.67	0.60	0.72	0.68	0.76	0.77	0.75	0.63	0.77	0.71	0.67	0.61	0.60	0.60
Al2O3	11.73	11.49	11.20	12.23	10.95	13.48	12.86	14.77	14.67	15.67	11.40	14.36	13.03	12.43	10.92	11.21	11.03
TFe2O3	4.49	4.29	4.20	4.67	4.05	5.43	5.04	5.73	5.77	6.09	4.38	5.71	5.17	4.91	4.15	4.21	4.19
MnO	0.09	0.08	0.08	0.08	0.07	0.10	0.09	0.105	0.10	0.10	0.08	0.11	0.10	0.09	0.08	0.08	0.08
MgO	2.59	2.56	2.40	2.35	2.24	2.13	2.07	2.09	2.06	1.91	2.39	2.11	2.08	2.23	2.65	2.73	2.80
CaO	7.49	7.45	8.39	5.24	7.98	6.04	7.40	2.60	1.21	1.02	9.56	1.12	5.47	7.13	8.39	8.56	8.16
Na2O	2.03	2.06	1.74	1.72	1.79	1.60	1.57	1.63	1.60	1.07	1.67	1.67	1.69	1.65	1.79	2.18	2.27
K2O	2.38	2.24	2.28	2.46	2.22	2.55	2.49	2.51	2.79	2.47	2.25	2.91	2.74	2.54	2.36	2.41	2.37
P2O5	0.15	0.14	0.14	0.11	0.13	0.13	0.14	0.14	0.14	0.07	0.13	0.19	0.16	0.15	0.14	0.15	0.15
LOI	8.94	10.20	9.48	7.54	8.67	8.80	9.83	7.33	5.18	6.39	10.58	4.30	8.06	8.97	9.12	9.58	10.28
TOTAL	102.00	101.36	100.83	102.12	101.23	102.35	101.12	102.72	101.41	100.87	102.13	101.66	101.74	100.23	100.91	100.57	100.60
Li	36.8	34.5	34.5	32.9	29.1	44.5	40.9	45.5	39.6	50.5	36.7	41.7	37.4	36.8	30.4	35.2	32.8
Be	2.04	1.77	1.96	1.80	1.53	2.38	2.17	2.22	3.04	2.55	1.94	2.64	2.17	1.94	1.57	1.83	1.71
Sc	11.3	11.6	10.9	10.4	11.0	13.0	12.6	13.8	14.3	15.1	11.1	14.1	12.7	12.7	11.3	10.9	11.4
V	82.5	73.5	80.9	74.9	65.8	98.8	94.7	104.4	105.5	109.5	82.7	101.9	92.8	81.1	68.9	79.6	71.8
Cr	68.5	66.1	65.2	60.1	58.0	74.0	72.6	79.4	77.3	83.4	65.1	75.2	72.1	67.6	66.8	69.2	65.6
Co	11.7	11.2	11.0	10.3	9.9	14.0	13.6	15.0	15.3	15.8	11.4	15.0	13.7	12.6	10.3	11.2	10.9
Ni	31.1	30.2	28.8	28.0	27.4	36.9	35.6	39.8	39.6	44.8	31.0	41.3	36.8	34.6	28.8	29.5	30.2
Cu	21.2	21.2	19.8	18.3	18.5	26.7	25.0	27.1	27.9	28.1	21.0	28.9	25.3	24.8	20.2	20.8	21.3
Zn	68.4	64.8	63.2	57.2	56.2	74.8	72.2	78.4	81.4	82.2	62.8	84.1	76.5	71.8	59.2	63.6	65.4
Ga	14.4	14.2	13.6	13.0	12.9	16.7	16.1	17.8	18.0	19.1	13.9	17.7	16.2	15.4	12.9	13.7	13.8
Rb	96.2	88.7	92.2	87.7	82.3	110.4	105.5	117.5	118	117	92.1	121.3	111.1	102.0	85.0	94.7	90.2
Sr	301	264	253	229	215	152	155	142	172	138	287	134	181	167	262	292	248
Y	24.3	24.2	25.7	24.3	22.5	28.9	27.2	31.4	32.6	29.4	25.9	32.7	28.7	25.2	23.5	25.7	24.6
Zr	220	222	229	242	221	221	214	230	241	251	218	254	238	198	251	236	211
Nb	13.0	12.4	12.6	11.7	11.8	14.2	13.9	15.3	15.6	15.1	12.3	15.6	14.2	13.1	11.8	12.0	12.0
Mo	1.22	0.73	0.61	0.61	0.61	0.88	0.87	0.90	0.88	1.10	0.79	0.91	0.85	0.80	1.02	0.96	0.99
Sn	2.47	2.56	2.53	2.29	2.35	3.01	2.75	3.11	3.13	3.26	2.44	3.22	2.82	2.89	2.36	2.46	2.59
Cs	7.13	6.62	6.42	5.92	5.64	9.13	8.62	9.60	9.64	10.48	6.86	9.76	8.61	7.96	5.77	6.49	6.31
Ba	523	480	476	485	445	555	533	575	589	565	494	571	536	497	469	501	480
La	32.1	31.7	31.4	31.5	28.3	38.1	36.7	39.4	40.4	38.5	33.3	41.4	36.8	34.5	29.2	31.3	32.4
Ce	65.1	64.1	62.8	63.6	57.2	77.5	73.7	80.2	82.1	82.3	67.3	82.1	75.0	69.1	59.2	63.7	65.4
Pr	7.37	7.36	7.21	7.31	6.62	8.79	8.41	8.98	9.31	9.02	7.73	9.45	8.58	7.88	6.84	7.26	7.50
Nd	27.4	27.8	26.6	27.5	25.1	32.7	30.9	33.2	34.0	32.8	28.7	34.9	31.2	30.0	25.9	27.1	28.2
Sm	5.44	5.46	5.32	5.48	4.96	6.51	6.14	6.62	6.86	6.66	5.73	6.99	6.31	5.93	5.20	5.54	5.59
Eu	1.08	1.11	1.06	1.03	1.00	1.24	1.18	1.27	1.36	1.32	1.10	1.34	1.22	1.17	1.05	1.07	1.08
Gd	4.84	5.03	5.03	4.98	4.69	5.76	5.58	6.02	6.15	5.86	5.41	6.42	5.67	5.39	4.80	5.08	5.26
Tb	0.73	0.71	0.76	0.75	0.67	0.88	0.83	0.93	0.96	0.91	0.80	0.97	0.87	0.76	0.68	0.77	0.75
Dy	4.26	4.48	4.37	4.30	4.17	5.06	4.66	5.18	5.61	5.16	4.56	5.50	5.06	4.80	4.33	4.44	4.62
Ho	0.88	0.88	0.93	0.90	0.84	1.06	0.99	1.11	1.18	1.10	0.94	1.15	1.05	0.94	0.87	0.93	0.91
Er	2.50	2.72	2.64	2.51	2.51	3.04	2.77	3.15	3.33	3.13	2.65	3.30	2.99	2.78	2.59	2.66	2.67
Tm	0.38	0.40	0.41	0.39	0.37	0.46	0.42	0.48	0.50	0.48	0.42	0.49	0.45	0.40	0.39	0.40	0.40

Yb	2.43	2.51	2.60	2.48	2.33	2.96	2.69	3.03	3.21	3.08	2.69	3.17	2.91	2.64	2.48	2.60	2.53
Lu	0.38	0.39	0.40	0.39	0.36	0.45	0.42	0.48	0.50	0.48	0.41	0.49	0.43	0.39	0.37	0.40	0.40
Hf	5.68	6.12	5.97	6.37	5.94	5.77	5.56	5.93	6.16	6.50	5.61	6.49	6.14	5.53	6.83	6.12	5.83
Ta	0.99	0.96	0.96	0.92	0.93	1.11	1.08	1.14	1.19	1.16	0.93	1.16	1.14	1.03	0.91	0.93	0.93
W	2.03	2.08	1.90	2.09	1.90	2.39	2.26	2.43	2.56	2.54	1.99	2.43	2.31	2.26	1.90	1.84	2.02
Pb	18.9	17.9	17.8	17.3	16.4	22.8	21.7	23.4	24.2	25.4	18.8	23.9	22.2	20.3	17.7	18.5	18.3
Th	11.4	11.0	10.9	11.4	10.0	13.8	13.3	14.0	14.3	14.9	11.7	14.3	13.2	12.5	10.6	11.6	11.7
U	3.22	3.64	2.72	2.71	2.42	2.59	2.49	2.62	2.59	3.78	3.25	2.79	2.82	2.46	3.36	3.17	3.20

	Jiuzhoutai Loess						
Location	36°5'N, 103°47'E						
Sample	JZT16-04a	JZT16-05a	JZT16-06a	JZT16-07a	JZT16-08a	JZT16-09a	JZT16-11a
SiO2	61.17	56.53	59.78	57.25	57.17	59.30	56.97
TiO2	0.60	0.58	0.59	0.59	0.62	0.66	0.65
Al2O3	11.00	10.65	10.64	10.90	11.29	11.97	11.69
TFe2O3	4.12	4.01	3.96	4.19	4.42	4.66	4.54
MnO	0.08	0.08	0.08	0.08	0.09	0.09	0.089
MgO	2.72	2.68	2.56	2.96	2.99	3.05	2.99
CaO	8.56	9.64	8.79	9.42	8.92	6.84	8.58
Na2O	1.86	1.74	1.82	1.91	1.72	2.19	2.14
K2O	2.31	2.31	2.35	2.32	2.40	2.50	2.17
P2O5	0.14	0.14	0.15	0.15	0.16	0.15	0.16
LOI	9.51	9.16	9.17	9.73	10.07	9.34	12.84
TOTAL	102.07	97.52	99.89	99.48	99.85	100.75	102.81
Li	30.7	34.4	31.2	37.3	35.8	38.8	38.1
Be	1.53	1.73	1.63	2.13	1.84	1.96	1.94
Sc	10.9	10.6	11.0	10.6	12.1	11.8	11.4
V	67.0	75.6	69.0	78.5	74.0	87.0	84.8
Cr	60.8	68.2	65.6	65.7	69.9	72.1	70.1
Co	10.1	10.3	10.2	10.9	11.5	12.3	11.9
Ni	28.0	28.1	28.9	29.6	31.7	33.5	32.4
Cu	19.8	20.0	20.3	20.6	22.3	24.2	23.0
Zn	58.0	59.1	60.1	62.7	68.5	81.5	69.7
Ga	12.9	13.0	13.4	13.5	14.3	14.8	14.4
Rb	85.2	90.5	87.6	93.9	93.6	103	98
Sr	275	420	267	343	335	237	297
Y	24.2	27.2	23.1	23.5	23.0	26.0	27.0
Zr	220	286	230	217	215	231	238
Nb	11.3	11.9	12.0	12.0	12.5	13.2	12.9
Mo	0.99	1.03	0.97	1.90	0.83	1.15	1.17
Sn	2.40	2.35	2.43	2.45	2.67	2.62	2.58
Cs	5.75	6.11	6.07	6.68	7.33	7.90	7.46
Ba	473	503	498	506	481	507	516
La	30.2	32.5	32.1	31.9	32.5	35.3	35.2
Ce	61.1	66.0	64.4	64.8	65.3	71.1	71.5
Pr	7.06	7.60	7.40	7.37	7.51	8.15	8.10
Nd	26.7	28.2	28.1	27.5	28.4	29.7	29.9
Sm	5.38	5.65	5.47	5.56	5.60	5.93	5.87
Eu	1.07	1.06	1.08	1.07	1.10	1.12	1.16
Gd	4.93	5.31	4.92	5.04	5.04	5.37	5.44
Tb	0.71	0.79	0.70	0.74	0.71	0.81	0.82
Dy	4.38	4.57	4.33	4.08	4.40	4.55	4.67
Ho	0.88	0.96	0.85	0.84	0.87	0.94	0.96
Er	2.66	2.82	2.52	2.38	2.54	2.67	2.75
Tm	0.38	0.46	0.37	0.36	0.37	0.41	0.42

Yb	2.52	2.97	2.37	2.31	2.46	2.62	2.64
Lu	0.38	0.47	0.36	0.35	0.37	0.40	0.41
Hf	5.96	7.15	6.25	5.54	5.93	5.95	6.09
Ta	0.85	0.92	0.94	0.93	0.96	1.12	0.99
W	1.85	1.82	1.85	2.09	2.07	2.22	2.18
Pb	17.1	18.1	17.7	18.4	19.1	20.4	20.4
Th	10.4	12.3	10.9	11.4	11.4	12.5	12.2
U	3.45	4.55	3.17	4.56	3.05	3.52	3.34

Supplementary Table 2 Strontium isotope composition of loess and paleosol samples from the Chinese Loess Plateau

			Rb ppm	Sr ppm	Rb/Sr	$^{87}Rb/^{86}Sr$	$^{87}Sr/^{86}Sr$	1 sigma
Leoss	Qin'an	16QA-01a	81	293	0.2770	0.8018	0.713080	0.000006
		16QA-02a	70	325	0.2146	0.6212	0.712474	0.000006
		16QA-04a	98	321	0.3060	0.8859	0.713980	0.000003
		16QA-05a	100	299	0.3328	0.9635	0.714082	0.000006
	Quaternary	16LC-03a	94	200	0.4728	1.3689	0.715690	0.000005
		16LC-07	108	154	0.7021	2.0335	0.718482	0.000005
		16LC-10a	103	175	0.5855	1.6956	0.717635	0.000006
		16HK-01a	90	313	0.2867	0.8301	0.713878	0.000005
		16HK-05B	92	253	0.3639	1.0535	0.714935	0.000006
		16YA-01a	88	229	0.3830	1.1091	0.716307	0.000005
		16LT-01a	92	287	0.3211	0.9297	0.714332	0.000005
		16LT-03a	111	181	0.6151	1.7813	0.717137	0.000006
		16LT-04A	102	167	0.6102	1.7672	0.716921	0.000004
		JZT16-06a	88	267	0.3275	0.9483	0.714537	0.000005
		JZT16-07a	94	343	0.2737	0.7924	0.713780	0.000004
		JZT16-08a	94	335	0.2791	0.8080	0.714134	0.000005
Paleosol		16LC-02a	114	174	0.6528	1.8904	0.716692	0.000005
		16LC-04a	116	183	0.6354	1.8400	0.717166	0.000005
		16LC-06a	117	145	0.8072	2.3380	0.719053	0.000005
		16LC-08a	114	156	0.7335	2.1244	0.718371	0.000005
		16LC-11a	105	139	0.7525	2.1795	0.718775	0.000004
		16LTN-04a	118	172	0.6861	1.9871	0.717532	0.000005
		16LTN-05a	117	138	0.8469	2.4531	0.718856	0.000005

Supplementary Table 3: Compiled geochemical data for global loess and paleosol samples in the literature (major elements in wt.%, trace elements in ppm)

	Chinese Loess Plateau (CLP) - Xining loess										CLP - Xifeng				
	XN-2 ChauvelEtAl2014EPSL	XN-4 ChauvelEtAl2014EPSL	XN-10 ChauvelEtAl2014EPSL	XN-6 ChauvelEtAl2014EPSL	XN-2 JahnEtAl2001C	XN-3 JahnEtAl2001C	XN-4 JahnEtAl2001C	XN-5 JahnEtAl2001CG	XN-6 JahnEtAl2001CG	XN-10 JahnEtAl2001C	XF-10 ChauvelEtAl2014EPSL	XF-6 ChauvelEtAl2014EPS	XF-2 ChauvelEtAl2014EPS	XF-4 ChauvelEtAl2014EPSL	XF-2 JahnEtAl2001C
SiO2					64.45	63.80	66.03	63.27	65.35	65.07					68.24
TiO2					0.65	0.66	0.63	0.71	0.65	0.64					0.76
Al2O3					12.49	12.67	12.01	13.24	12.35	12.31					13.47
Fe2O3					4.61	4.76	4.30	5.12	4.51	4.39					5.08
MnO					0.09	0.09	0.09	0.10	0.09	0.09					0.10
MgO					2.69	2.74	2.57	2.97	2.62	2.73					2.18
CaO					10.46	10.70	9.95	9.93	10.04	10.30					5.61
Na2O					1.85	1.84	1.85	1.79	1.76	1.84					1.84
K2O					2.58	2.59	2.42	2.69	2.49	2.47					2.57
P2O5					0.15	0.15	0.14	0.18	0.14	0.16					0.15
LOI															
Total					100.02	100.00	99.99	100.00	100.00	100.00					100.00
Li	37.5	36.3	38.1	39.7							40.0	39.9	38.0	35.5	
Be															
B															
Sc	11.4	10.9	10.8	11.6							12.4	12.8	12.2	11.5	
V	74.2	69.5	70.9	75.3							84.1	87.1	83.0	76.7	
Cr	64.9	66.8	60.5	70.6							76.9	79.9	73.2	71.4	
Co	10.9	10.1	10.1	11.1							12.3	13.0	12.1	11.0	
Ni	28.8	26.2	27.2	29.3							34.4	35.9	33.8	32.1	
Cu	22.6	19.7	19.5	21.7							25.3	26.1	23.8	34.1	
Zn	65.9	59.2	60.2	66.7							71.2	77.2	68.8	72.2	
Ga															
Ge															
As															
Rb	102	95.7	97.2	103	90	89	79	94	67	87	107	112	108	97.4	73
Sr	296	322	303	465	266	250	282	244	386	276	205	232	178	242	160
Y	28.1	28.8	27.2	28.4	22.10	14.50	20.90	23.10	21.40	19.90	31.0	31.1	29.5	29.4	27.80
Zr	208	269	237	282	122	146	144	136	142	117	238	245	155	250	241
Nb	12.3	12.4	12.3	13.2	11.30	11.30	11.10	11.90	11.10	10.40	13.8	14.5	13.1	13.1	11.90
Mo															
Cd															
In															
Sn															
Sb															
Cs	6.89	6.35	6.60	6.98	6.20	6.40	5.20	6.80	3.90	6.00	7.90	7.98	7.61	6.66	6.50
Ba	481	488	474	510	456	385	460	462	469	470	487	515	495	473	473
La	31.6	30.4	31.6	31.1	28.7	21.2	23.0	30.2	22.9	24.8	32.7	33.9	34.5	32.1	33.0
Ce	61.6	61.2	63.8	64.1	59.5	52.4	48.6	62.5	48.3	51.6	66.8	70.7	68.0	65.6	69.6
Pr	7.41	7.07	7.38	7.35	6.71	4.73	5.38	6.99	5.37	5.83	7.74	8.06	8.26	7.62	7.89
Nd	27.4	26.5	27.1	27.5	25.80	17.80	20.80	26.80	20.70	22.30	29.1	29.7	30.1	28.1	30.10
Sm	5.30	5.45	5.34	5.44	4.85	3.25	4.04	5.15	4.04	4.30	5.66	5.90	5.97	5.62	5.75
Eu	1.00	1.00	0.98	1.05	1.00	0.64	0.87	1.00	0.88	0.90	1.13	1.16	1.12	1.07	1.15
Gd	4.73	4.62	4.68	4.63	4.71	3.17	4.13	4.90	4.16	4.24	5.06	5.19	5.29	4.99	5.35
Tb	0.761	0.74	0.732	0.753	0.65	0.42	0.58	0.68	0.58	0.57	0.804	0.818	0.821	0.767	0.78
Dy	4.31	4.28	4.12	4.36	3.85	2.52	3.59	3.98	3.62	3.50	4.62	4.84	4.67	4.49	4.81
Ho	0.872	0.887	0.855	0.885	0.76	0.50	0.73	0.79	0.74	0.69	0.95	0.994	0.929	0.921	0.97
Er	2.58	2.63	2.53	2.59	2.11	1.39	2.04	2.38	2.07	2.01	2.82	2.86	2.66	2.67	2.76
Tm					0.31	0.20	0.30	0.33	0.31	0.29					0.40
Yb	2.39	2.44	2.32	2.48	1.98	1.34	1.95	2.06	1.96	1.88	2.57	2.71	2.54	2.51	2.62
Lu	0.371	0.387	0.365	0.39	0.31	0.21	0.31	0.34	0.32	0.30	0.41	0.416	0.385	0.394	0.43
Hf	4.88	6.23	5.68	6.62	3.10	3.70	3.70	3.50	3.60	3.00	5.75	5.84	4.06	5.89	6.10
Ta	1.14	0.87	0.88	0.978	0.87	0.95	0.96	0.92	0.83	0.79	0.98	1.02	1.01	0.921	0.89
W															
Tl	0.669	0.657	0.676	0.729							0.746	0.785	0.735	0.676	
Pb	18.7	17.9	18.1	19.4	16.50	16.60	16.30	18.90	17.00	15.50	20.1	20.7	20.6	18.7	17.50
Bi															
Th	11.6	10.8	11.4	11.3	10.30	7.30	8.40	10.00	8.50	8.50	12.3	12.5	12.6	12.1	11.20
U	2.94	3.10	2.80	3.66	2.71	3.15	2.91	3.88	3.22	2.52	2.60	2.63	2.35	2.48	2.37

	g loess					CLP - Jixian loess									
	XF-3 JahnEtAl2 001CG	XF-4 JahnEtAl2 001CG	XF-5 JahnEtAl2 001CG	XF-6 JahnEtAl2 001CG	XF-10 JahnEtAl2 001CG	JX-2 JahnEtAl2 001CG	JX-3 JahnEtAl2 001CG	JX-4 JahnEtAl2 001CG	JX-5 JahnEtAl2 001CG	JX-6 JahnEtAl2 001CG	JX-10 JahnEtAl2 001CG	JX-2 ChauvelEt Al2014EP	JX-4 ChauvelEt Al2014EP	JX-6 ChauvelEt Al2014EP	JX-10 ChauvelEt Al2014EP
SiO2	64.63	65.48	64.89	64.62	64.29	66.69	65.43	64.59	65.89	66.57	63.83				
TiO2	0.68	0.69	0.70	0.72	0.73	0.66	0.73	0.70	0.74	0.70	0.61				
Al2O3	12.96	12.76	13.28	13.50	13.61	12.49	13.60	13.06	13.64	12.61	11.56				
Fe2O3	4.85	4.75	5.03	5.15	5.25	4.48	5.18	4.96	5.20	4.63	4.09				
MnO	0.10	0.09	0.10	0.10	0.10	0.09	0.10	0.09	0.10	0.09	0.08				
MgO	2.42	2.40	2.47	2.63	2.48	2.18	2.49	2.39	2.30	2.40	1.93				
CaO	10.10	9.51	9.13	8.85	9.07	9.13	7.95	9.83	7.66	8.66	13.98				
Na2O	1.65	1.73	1.70	1.61	1.65	1.76	1.67	1.64	1.64	1.77	1.58				
K2O	2.46	2.44	2.55	2.63	2.63	2.37	2.67	2.56	2.67	2.42	2.20				
P2O5	0.16	0.15	0.16	0.18	0.18	0.14	0.18	0.17	0.18	0.15	0.14				
LOI															
Total	100.01	100.00	100.01	99.99	99.99	99.99	100.00	99.99	100.02	100.00	100.00				
Li												33.8	37.1	37.4	30.5
Be															
B															
Sc												11.4	12.0	11.8	10.8
V												74.3	81.5	77.2	70.0
Cr												69.2	74.0	74.4	64.4
Co												10.4	11.8	11.1	9.82
Ni												27.9	31.8	32.0	26.5
Cu												19.4	22.8	22.2	18.2
Zn												61.1	66.7	64.3	54.8
Ga															
Ge															
As															
Rb	89	91	94	77	91	77	81	91	90	88	72	93.7	102	97.9	85.4
Sr	210	232	215	203	188	212	167	174	156	212	213	235	192	231	246
Y	25.90	27.00	27.30	25.30	24.50	23.60	22.00	21.40	25.90	25.50	19.70	29.0	29.6	28.9	26.6
Zr	225	239	280	161	139	206	103	105	185	213	137	231	226	262	262
Nb	11.00	11.70	11.40	11.80	12.30	10.10	11.00	11.30	10.90	11.00	9.90	12.8	13.9	13.6	12.0
Mo															
Cd															
In															
Sn															
Sb															
Cs	6.30	6.30	6.70	6.60	6.60	5.40	6.30	6.70	6.90	6.20	4.60	6.30	7.43	6.79	5.65
Ba	477	483	481	462	484	432	478	448	464	448	389	442	464	459	414
La	30.7	31.8	31.8	29.4	30.9	29.1	32.6	31.0	31.5	30.8	26.5	30.0	32.2	32.3	27.5
Ce	63.7	66.4	66.4	63.6	64.7	60.3	67.3	63.8	65.9	64.0	54.6	60.6	65.0	65.3	56.9
Pr	7.27	7.52	7.43	7.05	7.21	6.80	7.59	7.20	7.41	7.18	6.19	7.16	7.57	7.58	6.57
Nd	27.80	28.80	28.60	27.30	27.70	26.30	29.10	27.70	28.40	27.50	23.70	26.7	28.2	28.3	24.3
Sm	5.29	5.39	5.34	5.21	5.16	4.90	5.36	5.17	5.33	5.19	4.46	5.25	5.61	5.56	4.67
Eu	1.08	1.09	1.10	1.09	1.10	1.01	1.08	1.05	1.11	1.05	0.91	1.05	1.09	1.05	0.92
Gd	5.00	5.14	5.06	5.08	5.10	4.62	4.95	4.68	5.06	4.92	4.13	4.67	4.97	4.87	4.22
Tb	0.73	0.74	0.73	0.70	0.70	0.67	0.69	0.66	0.73	0.72	0.58	0.745	0.79	0.753	0.701
Dy	4.42	4.61	4.49	4.27	4.21	4.05	3.96	3.84	4.44	4.34	3.52	4.33	4.41	4.35	3.95
Ho	0.89	0.92	0.91	0.86	0.85	0.83	0.78	0.76	0.90	0.88	0.69	0.908	0.908	0.900	0.838
Er	2.54	2.55	2.55	2.38	2.33	2.30	2.15	2.11	2.53	2.49	1.94	2.65	2.63	2.63	2.42
Tm	0.37	0.38	0.39	0.35	0.35	0.34	0.31	0.31	0.37	0.36	0.28				
Yb	2.40	2.53	2.59	2.33	2.27	2.26	2.07	2.03	2.44	2.40	1.84	2.44	2.48	2.50	2.35
Lu	0.40	0.40	0.39	0.36	0.35	0.35	0.32	0.32	0.39	0.38	0.30	0.389	0.387	0.379	0.365
Hf	5.60	5.90	6.80	4.20	3.70	5.20	2.80	2.80	4.80	5.50	3.60	5.65	5.56	6.28	6.14
Ta	0.85	0.94	0.84	0.88	0.92	0.83	0.89	0.93	0.90	6.34	0.79	0.904	0.97	0.943	0.837
W															
Tl												0.657	0.718	0.694	0.655
Pb	16.40	17.10	17.60	17.40	18.40	16.10	18.30	17.60	17.80	16.80	14.30	17.1	18.7	18.1	16.1
Bi															
Th	10.70	11.20	11.20	10.50	10.50	9.70	11.10	10.50	10.90	10.30	9.10	10.9	12.0	11.4	9.69
U	2.29	2.52	2.53	2.35	2.40	2.31	2.20	2.14	2.28	2.49	2.20	2.30	2.43	2.60	2.37

	CLP - Luochuan loess										CLP - Xining paleosol					
	L9 ChauvelEtAl2014EPS	6—4 GalletEtAl1996CG	27—3 GalletEtAl1996CG	40—2 GalletEtAl1996CG	51—1 GalletEtAl1996CG	59—3 GalletEtAl1996C	84—3 GalletEtAl1996C	95—3 GalletEtAl1996CG	107—2 GalletEtAl1996CG	115—2 GalletEtAl1996C	XN-1 JahnEtAl2001CG	XN-7 JahnEtAl2001CG	XN-8 JahnEtAl2001CG	XN-9 JahnEtAl2001CG	XF-1 JahnEtAl2001CG	XF-7 JahnEtAl2001CG
SiO2		58.51	58.79	58.20	59.85	57.52	57.80	60.36	59.71	63.17	62.36	64.25	61.63	66.44	67.42	64.57
TiO2		0.63	0.64	0.64	0.68	0.64	0.64	0.72	0.66	0.79	0.66	0.71	0.68	0.74	0.72	0.73
Al2O3		11.88	12.07	11.92	12.53	12.05	11.97	13.22	12.32	14.29	12.82	13.08	12.72	13.87	13.07	13.54
Fe2O3		4.49	4.57	4.55	4.82	4.59	4.57	5.15	4.70	5.65	4.80	4.98	4.87	5.29	4.87	5.19
MnO		0.08	0.09	0.08	0.09	0.08	0.09	0.10	0.08	0.11	0.09	0.10	0.09	0.11	0.10	0.10
MgO		2.19	2.12	2.07	2.12	2.07	2.00	2.16	2.19	2.21	2.60	2.77	3.02	2.59	2.27	2.51
CaO		8.53	8.23	8.31	6.67	8.69	8.49	6.01	7.27	2.89	12.22	9.49	12.62	6.14	6.96	8.89
Na2O		1.59	1.53	1.45	1.42	1.37	1.37	1.30	1.37	1.38	1.67	1.85	1.66	1.91	1.73	1.66
K2O		2.32	2.29	2.30	2.41	2.26	2.34	2.57	2.39	2.85	2.57	2.61	2.55	2.74	2.70	2.63
P2O5		0.15	0.14	0.16	0.14	0.15	0.17	0.16	0.16	0.12	0.20	0.16	0.16	0.16	0.16	0.18
LOI		9.26	9.21	9.20	8.17	9.78	9.57	8.19	8.95	6.25	12.57	9.35	11.63	7.65	7.79	8.78
Total		99.63	99.68	98.88	98.90	99.20	99.01	99.94	99.80	99.71	100	100	100	100	100	100
Li	37.9															
Be																
B																
Sc	10.9															
V	70.8															
Cr	63.7															
Co	10.2															
Ni	28.4															
Cu	20.8															
Zn	72.7															
Ga																
Ge																
As																
Rb	98	111	99	96	81	98	94	101			90	47	66	100	80	100
Sr	170	236	208	198	177	188	170	205			259	215	249	258	188	192
Y	27.7										21.80	20.80	16.80	24.50	26.50	28.30
Zr	216	205	182	192	206	163	190	186			119	139	167	129	231	219
Nb	12.1	10.8	6.8	11.6	12.3	10.6	12.3	11.8			11.20	11.80	11.20	12.20	11.60	12.00
Mo																
Cd																
In																
Sn																
Sb																
Cs	7.73	8.20	7.20	7.20	7.30	7.30	7.10	7.20			7.10	2.50	4.80	8.80	6.30	7.20
Ba	459	545.00	452.00	441.00	436.00	446.00	429.00	442.00			447	441	425	504	479	490
La	31.7	38.10	32.10	31.50	32.20	30.30	30.90	31.10			29.0	21.4	18.7	33.2	32.5	32.2
Ce	67.2	75.50	63.70	62.80	64.00	61.10	62.40	62.50			60.3	47.9	45.2	69.7	68.1	66.6
Pr	7.81	9.34	8.20	8.07	7.96	7.75	7.91	7.87			6.76	5.24	4.26	7.79	7.72	7.52
Nd	29.6	32.50	28.00	27.70	27.70	26.60	27.30	27.20			25.90	20.30	16.20	29.70	29.50	28.90
Sm	5.74	6.61	5.60	5.57	5.76	5.33	5.48	5.52			4.85	3.99	3.18	5.54	5.58	5.42
Eu	1.13	1.31	1.13	1.10	1.11	1.05	1.04	1.07			0.99	0.85	0.67	1.12	1.13	1.13
Gd	5.06	5.91	5.09	5.08	5.17	4.72	4.86	4.92			4.70	4.03	3.32	5.15	5.26	5.18
Tb	0.801	0.92	0.78	0.77	0.80	0.74	0.76	0.77			0.64	0.58	0.47	0.72	0.74	0.77
Dy	4.62	5.19	4.61	4.57	4.59	4.22	4.38	4.40			3.82	3.63	2.91	4.33	4.61	4.68
Ho	0.964	1.08	0.92	0.94	0.95	0.85	0.88	0.89			0.76	0.73	0.58	0.85	0.93	0.95
Er	2.78	2.97	2.61	2.60	2.72	2.37	2.47	2.52			2.08	2.08	1.66	2.42	2.65	2.69
Tm		0.49	0.44	0.43	0.44	0.39	0.41	0.41			0.30	0.31	0.24	0.35	0.39	0.40
Yb	2.63	3.03	2.74	2.72	2.78	2.47	2.55	2.60			1.98	1.97	1.56	2.22	2.53	2.64
Lu	0.405	0.45	0.42	0.40	0.41	0.38	0.40	0.40			0.31	0.32	0.25	0.35	0.41	0.41
Hf	5.61	5.34	4.79	5.11	5.37	4.39	5.09	4.95			3.10	3.70	4.20	3.40	6.00	5.50
Ta	0.971	0.87	0.47	0.89	1.06	0.80	0.96	0.94			0.89	0.93	0.84	0.91	0.89	0.90
W																
Tl	0.755															
Pb	19.5	23.00	20.00	20.00	23.00	20.00	20.00	21.00			17.20	16.80	16.00	19.10	17.20	18.20
Bi																
Th	11.6	14.30	11.90	11.90	13.00	11.20	11.50	11.90			10.30	8.10	7.60	11.90	10.90	11.50
U	2.52	2.93	2.94	2.84	2.69	2.58	2.66	2.65			2.38	3.09	3.24	3.26	2.46	2.46

			CLP - Jixian paleosol				CLP - Luochuan paleosol								
	XF-8 JahnEtAl 2001CG	XF-9 JahnEtA l2001C	JX-1 JahnEtA l2001C	JX-7 JahnEtA l2001C	JX-8 JahnEtAl 2001CG	JX-9 JahnEtAl 2001CG	18—1 GalletEtAl 1996CG	32—3 GalletEtAl 1996CG	47—3 GalletEtAl 1996CG	58—3 GalletEtAl 1996CG	71—2 GalletEtAl 1996CG	91—2 GalletEtAl 1996CG	97—2 GalletEtAl 1996CG	LO94 ChauvelEtA l2014EPSL	P2E1 ChauvelEtA l2014EPSL
SiO2	66.19	64.13	71.25	68.31	70.12	67.96									
TiO2	0.71	0.72	0.79	0.81	0.85	0.80									
Al2O3	13.26	13.67	14.55	14.36	14.74	14.23									
Fe2O3	4.99	5.28	5.40	5.49	5.64	5.44									
MnO	0.10	0.10	0.11	0.10	0.10	0.10									
MgO	2.35	2.48	1.79	2.25	2.16	2.25									
CaO	8.03	9.18	1.52	4.22	2.12	4.79									
Na2O	1.66	1.64	1.70	1.61	1.49	1.60									
K2O	2.57	2.63	2.73	2.72	2.68	2.69									
P2O5	0.15	0.18	0.15	0.14	0.11	0.14									
LOI	8.41	9.10	4.17	6.24	5.11	6.63									
Total	100	100	100	100	100	100									
Li														61.3	59.9
Be															
B															
Sc														8.73	8.63
V														85.2	83.5
Cr														69.4	67.4
Co														8.85	8.96
Ni														25.3	26.7
Cu														17.1	17.6
Zn														108	69.4
Ga															
Ge															
As															
Rb	94	83	95	97	65	102	86.00	88.00	53.00	93.00	41.00	96.00	95.00	63.7	65.6
Sr	194	193	126	145	123	151	112.00	135.00	117.00	123.00	64.00	153.00	178.00	133	135
Y	26.30	25.20	27.70	24.40	24.40	26.60	31.50	32.20	30.50	32.00	19.60	53.50	29.80	21.8	21.7
Zr	201	119	222	118	190	126	207.00	210.00	214.00	230.00	184.00	171.00	159.00	213	263
Nb	11.50	12.10	11.40	11.20	13.20	13.40	15.10	9.90	12.70	10.90	6.70	12.70	11.90	11.6	12.3
Mo															
Cd															
In															
Sn															
Sb															
Cs	6.40	7.40	7.50	7.70	7.70	7.80	9.10	9.10	7.60	7.90	7.10	7.70	7.40	3.87	3.73
Ba	473	496	502	501	499	502	198.00	494.00	396.00	494.00	412.00	454.00	434.00	510	557
La	31.2	33.3	34.1	34.9	27.4	34.2	33.30	34.20	31.40	35.10	15.80	49.10	34.60	27.5	26.4
Ce	65.4	69.0	71.8	72.0	64.7	71.1	47.20	52.30	47.00	67.70	36.10	68.10	62.30	61.5	60.6
Pr	7.33	7.71	7.98	8.05	6.71	8.06	8.69	8.92	8.18	8.67	4.32	11.91	8.66	6.83	6.62
Nd	28.20	29.80	30.60	30.90	26.00	30.90	0.40	31.40	28.70	30.50	15.40	44.40	29.50	25.5	24.6
Sm	5.26	5.53	5.74	5.80	5.03	5.78	6.09	6.38	5.80	6.40	3.32	9.84	5.79	4.86	4.70
Eu	1.08	1.16	1.20	1.16	1.02	1.21	1.21	1.25	1.12	1.22	0.67	2.06	1.17	1.03	1.02
Gd	5.05	5.14	5.34	5.19	4.71	5.28	5.48	5.68	5.22	5.63	3.21	9.86	5.24	4.20	4.06
Tb	0.71	0.74	0.80	0.73	0.70	0.79	0.85	0.89	0.81	0.87	0.51	1.52	0.80	0.647	0.625
Dy	4.40	4.39	4.81	4.27	4.25	4.67	4.93	5.17	4.77	4.87	3.20	8.71	4.68	3.88	3.76
Ho	0.89	0.88	0.97	0.85	0.86	0.93	0.99	1.04	0.96	1.02	0.66	1.78	0.95	0.818	0.787
Er	2.49	2.43	2.74	2.35	2.43	2.62	2.79	2.93	2.69	2.96	1.91	4.87	2.62	2.43	2.34
Tm	0.38	0.36	0.40	0.34	0.36	0.38	0.47	0.49	0.45	0.46	0.32	0.73	0.44		
Yb	2.49	2.39	2.62	2.27	2.38	2.45	2.97	3.06	2.84	2.93	2.11	4.38	2.73	2.42	2.28
Lu	0.39	0.36	0.41	0.35	0.38	0.38	0.45	0.48	0.45	0.44	0.32	0.62	0.40	0.378	0.353
Hf	5.20	3.30	5.60	3.20	5.00	3.40	5.60	5.72	5.84	6.15	4.98	4.60	4.17	5.92	6.98
Ta	0.87	0.95	0.90	0.94	1.09	1.03	1.19	0.85	1.04	1.00	0.35	0.99	0.87	0.881	0.901
W															
Tl														0.569	0.585
Pb	17.60	18.80	20.00	19.60	20.50	19.40	22.00	22.00	21.00	23.00	15.00	21.00	21.00	15.4	15.7
Bi															
Th	10.90	11.70	11.70	11.80	9.60	12.20	12.80	12.60	12.40	14.00	55.00	13.10	11.40	7.85	7.64
U	2.41	2.21	2.30	2.33	2.55	2.40	2.06	2.27	2.15	2.66	1.10	2.58	2.47	2.19	2.11

	Spitsbergen (Svalbard)						England		Belgium					
	P2E1 GalletEtAl 1998EPS	P2E2 GalletEtAl 1998EPS	P2E3 GalletEtAl 1998EPS	LO94 GalletEtAl 1998EPS	GAI GalletEtAl 1998EPS	2408M3 GalletEtAl 1998EPS	SCIL ChauvelEtA l2014EPSL	SCIL GalletEtAl 1998EPS	K14 ChauvelEtA l2014EPSL	R11 ChauvelEtA l2014EPSL	R11dup ChauvelEtA l2014EPSL	PR GalletEtAl19 98EPSL	PR-RT ChauvelEtA l2014EPSL	HOT GalletEtAl1 998EPSL
SiO2	76.66	76.85	76.65	78.73	78.66	76.98		83.94				77.72		75.59
TiO2	0.70	0.74	0.75	0.61	0.60	0.72		0.57				0.44		0.70
Al2O3	12.50	12.32	12.41	10.85	10.94	12.17		8.50				6.23		8.34
Fe2O3	4.80	4.75	4.91	3.52	3.51	4.83		2.80				1.96		2.99
MnO	0.04	0.03	0.03	0.04	0.04	0.03		0.05				0.04		0.04
MgO	0.77	0.75	0.74	1.04	1.03	0.72		0.59				1.11		1.42
CaO	0.45	0.41	0.43	0.56	0.55	0.43		0.46				9.71		7.83
Na2O	1.43	1.54	1.41	2.20	2.22	1.56		0.96				0.97		1.12
K2O	2.49	2.44	2.49	2.37	2.36	2.40		2.05				1.70		1.86
P2O5	0.15	0.17	0.17	0.10	0.09	0.16		0.07				0.11		0.11
LOI														
Total														
Li							41.1		30.9	44.6	44.5		17.9	
Be														
B														
Sc							6.46		10.9	10.3	10.5		6.01	
V							39.2		53.9	58.3	58.8		28.4	
Cr							61.4		95.4	105	112		50.9	
Co							6.21		8.79	7.90	8.05		4.20	
Ni	25.00	29.00	27.00	27.00	10.00	27.00	18.0	20.00	21.0	23.1	23.3	15.00	13.6	19.00
Cu							7.62		10.2	10.2	10.3		6.38	
Zn							42.8		58.0	54.0	43.3		25.3	
Ga														
Ge														
As														
Rb	81.00			82.00		77.00	68.4		84.6	71.8	73.8	52.00	47.4	62.00
Sr	159.00			156.00		157.00	64.2	75.00	83.2	66.5	68.2	197.00	190	174.00
Y	23.70			22.60		23.00	16.9		34.1	31.5	32.1	18.10	19.3	29.20
Zr	303.00	272.00	291.00	243.00	261.00	300.00	356	327.00	593	620	622	307.00	343	367.00
Nb	15.00			14.00		13.50	10.2		15.9	17.6	17.5	7.90	7.77	11.70
Mo														
Cd														
In														
Sn														
Sb														
Cs							4.28		3.83	3.51	3.53		2.18	
Ba	567			519		536	292		373	350	352	246	245	297
La	29.70			29.30		28.80	19.0	19.66	34.5	34.9	34.3	19.5	19.7	26.7
Ce	63.40			62.30		60.40	43.2	42.95	76.3	76.4	74.4	39.6	41.3	54.6
Pr	7.70			7.70		7.40	4.70	4.40	9.04	8.61	8.50	5.30	5.10	7.10
Nd	26.90			26.30		25.60	16.9	16.83	34.4	32.2	31.3	18.70	19.3	25.0
Sm	5.20			5.02		4.84	3.20	3.14	6.83	6.16	5.81	3.78	3.9	5.06
Eu	1.10			1.07		1.05	0.592	0.57	1.26	1.08	1.08	0.72	0.667	0.98
Gd	4.44			4.24		4.24	2.75	3.00	5.99	5.34	5.25	3.41	3.33	4.62
Tb	0.69			0.66		0.65	0.445	0.41	0.938	0.842	0.831	0.51	0.518	0.74
Dy	3.87			3.65		3.68	2.74	1.98	5.52	5.14	5.17	2.90	3.05	4.41
Ho	0.81			0.76		0.78	0.593	0.40	1.16	1.10	1.11	0.58	0.626	0.92
Er	2.16			2.09		2.13	1.77	1.09	3.33	3.24	3.35	1.56	1.85	2.59
Tm	0.36			0.34		0.35		1.18				0.25		0.44
Yb	2.31			2.15		2.24	1.86		3.38	3.33	3.37	1.66	1.82	2.81
Lu	0.36			0.34		0.36	0.295	0.18	0.524	0.519	0.537	0.25	0.286	0.43
Hf							9.02		14.6	16.3	16.1		8.5	
Ta	1.00			0.90		0.90	0.857		1.23	1.41	1.37	0.60	0.647	1.40
W														
Tl							0.591		0.665	0.617	0.609		0.412	
Pb	18.80			18.10		17.90	14.1		16.6	15.8	16.0	10.70	10.0	13.10
Bi														
Th	9.70			8.70		8.50	7.40		9.99	10.5	10.7	6.40	6.44	8.30
U	2.52			2.43		2.21	1.84		2.38	2.63	2.74	1.60	1.80	2.32

	France											
	HOT1-WholeRock ChauvelEtAl2014EPSL	HOT1<160mm ChauvelEtAl2014EPSL	FOUG3 GalletEtAl 1998EPS	FOUG3a<160mm ChauvelEtAl2014 EPSL	HC90/1 GalletEtAl1998EPSL	SAB1 GalletEtAl1998EPSL	SAB1a<160mm ChauvelEtAl2014EPSL	NS2 GalletEtAl 1998EPSL	NS3 GalletEtAl1998EPSL	NS4 GalletEtAl1998EPSL	NS6 GalletEtAl 1998EPSL	NS6<160mm ChauvelEtAl2014EPSL
SiO2			84.74		76.00	80.56		59.34	77.46	71.56	75.07	
TiO2			0.87		0.78	0.37		0.79	0.78	0.93	0.97	
Al2O3			8.51		8.23	6.45		9.84	11.09	10.59	10.65	
Fe2O3			2.47		3.20	1.83		4.34	4.42	5.05	4.51	
MnO			0.02		0.05	0.03		0.06	0.07	0.08	0.06	
MgO			0.36		1.16	0.99		0.92	0.88	1.21	1.29	
CaO			0.28		7.76	7.00		21.46	1.14	7.05	3.93	
Na2O			0.93		0.78	0.99		1.59	1.89	1.56	1.51	
K2O			1.76		1.92	1.70		1.55	2.16	1.82	1.89	
P2O5			0.05		0.12	0.09		0.11	0.10	0.14	0.12	
LOI												
Total												
Li	25.8	23.9		29.6			16.6					29.6
Be												
B												
Sc	8.33	7.71		8.73			4.55					10.6
V	46.8	41.8		43.9			26.0					68.0
Cr	61.3	62.5		76.0			35.4					68.5
Co	6.09	4.87		3.80			3.97					7.66
Ni	16.7	15.3	7.00	10.3	22.00	12.00	11.6	12.00	16.00	24.00	21.00	18.9
Cu	9.04	8.4		4.95			6.33					11.5
Zn	38.5	34.3		38.5			36.7					50.7
Ga												
Ge												
As												
Rb	58.3	56.8	62.00	61.0	64.00	54.00	50.8				68.00	64.5
Sr	167	167	59.00	62.8	150.00	152.00	170				131.00	131
Y	27.4	24.4	20.60	33.1	28.80	15.10	14.0				28.00	31.1
Zr	408	387	468.00	562	487.00	223.00	193	149.00	161.00	305.00	342.00	411
Nb	10.9	10.2	14.70	15.4	8.60	6.10	5.78				12.40	11.8
Mo												
Cd												
In												
Sn												
Sb												
Cs	3.25	2.90		3.03			1.93					3.48
Ba	301	281	301	299	282	277	277				329	324
La	25.2	23.4	28.4	28.2	29.5	14.8	13.8				30.4	28.3
Ce	53.6	47.6	60.7	67.7	59.7	29.9	28.4				60.5	60.5
Pr	6.43	5.98	7.30	7.30	7.80	4.00	3.58				8.00	7.20
Nd	24.5	22.7	25.6	27.4	27.5	14.3	13.9				28.4	27.6
Sm	4.94	4.48	4.97	5.38	5.59	2.99	2.70				5.67	5.55
Eu	0.938	0.852	0.83	0.854	1.03	0.61	0.562				1.13	1.07
Gd	4.44	4.07	4.14	4.80	4.99	2.68	2.35				5.04	5.01
Tb	0.706	0.64	0.64	0.784	0.78	0.41	0.362				0.79	0.805
Dy	4.31	3.91	3.50	4.90	4.53	2.43	2.21				4.53	4.98
Ho	0.93	0.808	0.71	1.06	0.93	0.49	0.455				0.89	1.05
Er	2.70	2.39	1.97	3.21	2.53	1.29	1.31				2.49	3.07
Tm			0.33		0.43	0.21					0.40	
Yb	2.69	2.33	2.14	3.23	2.78	1.40	1.29				2.59	3.01
Lu	0.421	0.363	0.33	0.511	0.42	0.21	0.199				0.39	0.461
Hf	10.4	9.51		13.5			4.60					10.3
Ta	0.892	0.815	1.10	1.20	0.70	0.40	0.473				1.00	0.958
W												
Tl	0.512	0.478		0.572			0.416					0.568
Pb	12.3	11.0	15.50	14.2	13.80	10.70	9.68				14.70	12.5
Bi												
Th	7.73	7.45	9.70	9.26	9.20	4.70	4.34				9.00	8.63
U	2.17	2.00	2.54	2.76	2.34	1.18	1.16				2.01	2.25

	Argentina, South America												Sahara, Africa	
	4—6 GalletEtAl1998EP	12—14 GalletEtAl1998EP	24—26 GalletEtAl1998EP	32—34 GalletEtAl1998EP	40—42 GalletEtAl1998EP	52—54 GalletEtAl1998EP	LUJA GalletEtAl1998EP	12-14 ChauvelEtAl2014EPS	24-26 ChauvelEtAl2014EPS	32RT ChauvelEtAl2014EPS	40RT ChauvelEtAl2014EPS	LUJA ChauvelEtAl2014EPS	Sample Meylan ChauvelEtAl2014EPSL	Sample 2900m ChauvelEtAl2014EPSL
SiO2	65.02	70.66	62.39	65.63	66.94	69.50	70.22							
TiO2	0.68	0.74	0.72	0.89	0.91	1.09	0.67							
Al2O3	15.14	14.41	15.01	16.91	16.20	13.59	15.40							
Fe2O3	4.81	4.34	4.67	5.58	5.64	5.33	3.58							
MnO	0.08	0.11	0.12	0.10	0.10	0.32	0.05							
MgO	1.54	1.10	1.35	1.67	2.15	1.56	1.36							
CaO	8.41	3.41	10.94	4.19	3.55	4.84	2.60							
Na2O	1.99	2.67	2.44	2.60	1.93	1.50	3.36							
K2O	2.18	2.37	2.12	2.28	2.44	2.14	2.65							
P2O5	0.16	0.18	0.23	0.15	0.14	0.14	0.10							
LOI														
Total														
Li								26.3	26.1	31.8	36.7	30.6	48.7	56.5
Be														
B														
Sc								10.9	11.9	13.6	14.0	10.0	13.0	12.3
V								82.2	85.9	107	94.8	73.6	102	106
Cr								34.1	28.8	35.6	36.1	30.1	87.3	95.6
Co								9.79	10.3	10.0	10.2	5.85	14.2	13.4
Ni	9.00	39.00	9.00	13.00	14.00	19.00	7.00	71.8	11.4	12.7	15.2	8.77	36.0	40.3
Cu								28.9	23.8	27.0	35.3	16.4	40.1	38.4
Zn								70.1	66.6	69.3	79.1	54.7	138	116
Ga														
Ge														
As														
Rb	76.00	81.00	68.00	76.00	82.00	82.00	90.00	79.5	77.2	64.6	68.8	85.5	87.7	67.4
Sr	261.00	292.00	326.00	371.00	285.00	246.00	330.00	314	375	358	301	330	298	95.5
Y	21.10	22.50	21.80	25.40	23.60	28.10	20.50	25.3	29.3	29.8	26.6	25.6	37.2	33.3
Zr	186.00	252.00	201.00	232.00	225.00	290.00	252.00	257	213	247	253	269	270	202
Nb	8.10	9.70	8.10	9.40	10.70	14.90	9.50	10.1	8.56	10.1	11.1	10.3	22.9	23.3
Mo														
Cd														
In														
Sn														
Sb														
Cs								4.62	4.32	4.70	5.76	4.58	4.33	4.95
Ba	504	543	565	600	423	890	524	555	572	643	480	579	552	363
La	21.3	23.2	21.4	22.5	25.1	30.1	23.5	23.3	22.7	23.9	24.7	21.8	41.8	37.7
Ce	41.0	47.1	42.3	46.5	52.2	69.5	46.8	47.3	45.1	48.9	52.6	45.4	84.7	79.1
Pr	5.60	6.20	5.80	6.40	6.90	8.20	6.40	5.87	5.9	6.31	6.57	5.57	10.1	9.35
Nd	20.4	21.9	21.4	23.4	24.7	29.0	22.6	22.1	22.9	24.8	25.1	21.2	37.9	34.7
Sm	4.23	4.43	4.44	4.89	5.20	5.80	4.46	4.39	4.74	5.18	5.25	4.30	7.28	6.68
Eu	1.01	1.03	1.06	1.25	1.16	1.30	1.02	1.01	1.10	1.22	1.18	0.997	1.49	1.31
Gd	3.68	3.96	3.90	4.44	4.50	5.12	3.80	3.96	4.19	4.64	4.53	3.79	6.31	5.61
Tb	0.56	0.60	0.59	0.67	0.68	0.79	0.58	0.609	0.693	0.731	0.711	0.617	0.988	0.902
Dy	3.16	3.51	3.37	4.05	3.81	4.61	3.37	3.71	4.26	4.35	4.20	3.71	5.73	5.11
Ho	0.66	0.75	0.71	0.82	0.78	0.92	0.68	0.788	0.887	0.905	0.849	0.779	1.16	1.04
Er	1.85	2.07	1.92	2.26	2.20	2.51	1.84	2.34	2.6	2.66	2.47	2.36	3.36	2.97
Tm	0.29	0.34	0.30	0.37	0.35	0.41	0.31							
Yb	1.91	2.13	2.00	2.42	2.17	2.69	2.04	2.30	2.51	2.57	2.30	2.32	3.03	2.80
Lu	0.28	0.34	0.30	0.36	0.25	0.40	0.31	0.35	0.394	0.399	0.358	0.361	0.47	0.427
Hf								6.04	4.90	5.75	6.00	6.34	6.53	4.96
Ta	0.70	0.80	0.60	0.70	0.90	1.10	0.80	0.732	0.579	0.685	0.758	0.755	1.48	1.67
W														
Tl								0.733	0.645	0.713	0.798	0.743	0.662	0.772
Pb	14.80	20.80	16.30	16.70	18.20	25.80	15.80	19.7	15.2	13.6	13.8	13.5	26.0	42.2
Bi														
Th	7.70	9.30	7.40	7.80	9.80	9.40	9.70	9.16	7.75	8.29	9.22	9.48	12.0	12.2
U	1.62	2.25	2.06	1.72	1.91	2.14	2.30	2.25	2.26	1.58	1.76	2.16	3.1	3.57

	Tadjikistan										Kansas		
	TJK2772 ChauvelEtAl2014EPSL	TJK2773 ChauvelEtAl2014EPSL	TJK2930 ChauvelEtAl2014EPSL	TJK3012 ChauvelEtAl2014EPSL	TJK3070 ChauvelEtAl2014EPSL	TJK3148 ChauvelEtAl2014EPSL	TJK3179 ChauvelEtAl2014EPSL	TJK3198 ChauvelEtAl2014EPSL	TJK2814 ChauvelEtAl2014EPSL	TJK3165 ChauvelEtAl2014EPSL	CY-4a-A Hu&Gao2008CG	CY-4a-B Hu&Gao2008CG	BP-1 Hu&Gao2008CG
SiO2											80.4	80.8	72.7
TiO2											0.64	0.63	0.57
Al2O3											10.5	10.6	15.8
Fe2O3											2.58	2.64	3.30
MnO											0.04	0.04	0.051
MgO											0.86	0.88	0.95
CaO											1.12	1.23	1.54
Na2O											1.58	1.68	3.27
K2O											2.53	2.62	2.39
P2O5													
LOI													
Total													
Li	44.3	43.0	35.6	46.7	35.4	37.8	55.2	32.5	36.5	45.8	15.7	17.9	32.1
Be											1.65	1.66	2.85
B											42.5	40.3	30.4
Sc	14.8	14.6	12.4	16.0	13.0	13.0	16.4	11.7	13.2	12.7	6.89	6.78	8.4
V	113	111	88.9	123	99.0	98.9	131	82.6	97	117	60	61.2	67
Cr	96.7	95.1	79.9	103	85.7	82.4	107	72.7	87.5	96.9	42.8	42.9	35.9
Co	15.4	15.1	12.5	17.2	13.8	14.0	17.9	12.6	14.0	16.4	5.77	5.97	11.3
Ni	51.6	51.2	42.8	57.3	43.8	43.8	59.9	38.5	44.2	51.7	14	15	15.3
Cu	33.5	34.4	26.8	37.8	29.0	30.1	41.8	24.9	29.5	34.8	12	12.3	14
Zn	89.6	86.3	72.3	98.2	81.3	84.4	111	72.4	79.7	98.3	40.1	40.9	67.9
Ga											11.3	11.5	14.5
Ge											1.43	1.4	1.44
As											3.87	3.74	4.11
Rb	114	112	93.2	93.1	97.7	101	119	91.0	93.6	126	82.1	83.5	95.7
Sr	193	208	280	149	209	228	135	229	276	161	204	207	314
Y	31.9	32.5	29.1	35.7	27.5	28.4	36.7	26.6	28.6	28.6	35	29.8	23.7
Zr	208	206	195	232	178	178	232	169	194	213	589	573	342
Nb	14.2	13.9	12.7	15.9	12.3	12.7	16.6	12.0	13.0	16.1	14.6	15	10.8
Mo											0.82	0.94	0.34
Cd											0.17	0.17	0.023
In											0.032	0.032	0.042
Sn											1.4	1.43	2.18
Sb											0.73	0.76	0.34
Cs	6.83	6.65	5.32	7.07	5.70	6.22	8.24	5.37	5.57	7.07	2.95	3.05	4.48
Ba	515	492	438	497	472	487	570	446	451	571	679	692	548
La	32.4	32.7	30.9	37.1	28.5	30.4	37.6	29.7	30.1	31.8	39.7	35.2	35.3
Ce	67.5	65.9	61.4	76.2	58.7	60.5	79.5	57.4	62.1	73.5	78.7	69.3	72.9
Pr	7.64	7.77	7.25	9.15	6.84	7.09	8.80	6.84	7.09	7.41	9.48	8.37	8.58
Nd	29.1	29.0	27.0	34.5	25.5	26.4	33.3	25.5	26.6	27.6	35.3	31.3	32.2
Sm	5.670	5.82	5.27	6.97	4.99	5.27	6.51	5.03	5.20	5.24	6.56	5.92	6.13
Eu	1.13	1.19	1.03	1.41	1.02	1.06	1.31	0.97	1.10	1.08	1.27	1.23	1.33
Gd	5.01	5.21	4.68	6.11	4.42	4.58	5.90	4.40	4.69	4.68	5.66	5.13	5.05
Tb	0.807	0.840	0.744	0.969	0.717	0.740	0.965	0.706	0.770	0.765	0.9	0.8	0.74
Dy	4.82	4.82	4.33	5.61	4.10	4.30	5.59	3.99	4.26	4.36	5.49	4.85	4.2
Ho	0.981	1.00	0.880	1.13	0.849	0.875	1.130	0.796	0.887	0.919	1.19	1.02	0.85
Er	2.85	2.92	2.52	3.22	2.44	2.50	3.34	2.30	2.56	2.62	3.5	2.98	2.39
Tm											0.58	0.5	0.38
Yb	2.69	2.74	2.37	3.00	2.24	2.40	3.09	2.18	2.41	2.46	3.66	3.19	2.4
Lu	0.408	0.421	0.364	0.458	0.349	0.360	0.478	0.333	0.375	0.386	0.58	0.51	0.38
Hf	5.02	4.95	4.62	5.58	4.32	4.29	5.55	4.12	4.66	5.18	14.9	14.4	8.85
Ta	1.01	1.02	0.930	1.13	0.883	0.923	1.18	0.873	0.890	1.13	1.01	1.05	0.89
W											1.26	1.32	1.41
Tl	0.751	0.740	0.631	0.787	0.642	0.667	0.892	0.629	0.656	0.857	0.6	0.61	0.64
Pb	21.4	20.6	18.4	18.1	18.7	19.5	24.2	18.6	18.1	22.8	15.3	16.2	15.7
Bi											0.16	0.16	0.19
Th	12.1	11.3	11.5	13.1	10.9	11.2	14.1	11.0	11.0	13.3	13.4	11.8	11
U	3.38	3.30	2.61	2.61	2.54	2.56	3.19	2.66	2.68	2.75	3.27	3.1	2.86

	Banks Penn., New Zealand						CN		Kaiserstuhl			Hungary	Kansas			Iowa
	BP-2		BP-3	BP-4		BP-5	Nanking	CH	1	2+		H	Kansas A	Kansas B	Kansas C	Iowa
	TayloEtAl1983GC	Barth2000CG	Hu&Gao2008C	TayloEtAl1983	Barth2000CG	Hu&Gao2008C	TayloEtAl1983GCA	Hu&Gao2008C	Hu&Gao2008C	TayloEtAl1983GC	Barth 2000	Hu&Gao2008C	TayloEtAl1983GCA	TayloEtAl1983GCA	TayloEtAl1983GCA	TayloEtAl1983GCA
SiO2	74.00		72.5	74.0		72.5	72.8		59.9	59.1			80.40	80.80	79.90	79.50
TiO2	0.55		0.69	0.57		0.54	0.78		0.32	0.29			0.64	0.63	0.71	0.69
Al2O3	14.70		15.2	14.30		15.1	15.4	13.18	7.78	7.98			10.5	10.6	10.7	11.40
Fe2O3	3.38		3.95	3.45		3.21	4.79	4.70	3.22	2.95			2.58	2.65	2.55	3.01
MnO	0.054		0.054	0.055		0.052	0.12		0.07	0.070			0.044	0.045	0.043	
MgO	0.97		0.88	1.07		1.06	1.59		3.45	4.37			0.86	0.95	0.88	1.01
CaO	1.47		1.27	1.27		1.58	0.95		23.11	22.90			1.12	1.09	1.23	0.85
Na2O	3.05		3.13	3.43		3.55	1.28		0.84	0.87			1.58	1.60	1.68	1.45
K2O	2.31		2.26	2.42		2.47	2.21		1.27	1.34			2.53	2.57	2.62	2.18
P2O5																
LOI													2.32	2.38	2.29	
Total													2.58	2.65	2.55	
Li	31		26.94	35		38.8	38	39.2	21.1			20.8				21
Be	2.3		2.43	2.2		2.44	2.4	2.19	1.19	1.1		1.6	1.4	1.5	1.4	1.4
B			34.9			38.8		71.4	55.7			69.3				
Sc	8.4		10.8	8.0		8.29	11.9	12.6	7.21	6.0		9.22	5.7	5.4	4.9	
V	63		66.5	65		65.1	99	85.2	42.5	39		61.8	55	57	57	
Cr	32		35.4	30		34.2	69	70.1	58.4	42		59.1	31	33	32	
Co	11		8.8	8		7.98	18	12.6	6.62	6		8.37	5	7	5	
Ni	14		12.3	13		15.3	34	35.5	26.2	23		26.6	13	13	11	
Cu	12		14.2	12		13.2	30	25	14.6	13		18	10	12	10	
Zn	54		51.3	53		47.5	78	64.2	36	35		48	46	45	44	
Ga	14	16.70	15.6	15	16.70	14.3	17	14.7	7.19	6.6	6.80	10.4	10	10	10	
Ge			1.51			1.39		1.52	1.07			1.29				
As			4.21			4.26		13.9	8.51			7.79				
Rb	86.7		84.4	84.2		96.8	108	104	47.9	49.7		68.8	74.2		71.9	77.00
Sr	310	304	318	275	276	323	104	230	396	302	300	195	187	205	195	162
Y	23	26.5	30.8	23	26.3	21.2	26.0	30.4	25	19.00	28.80	29.1	22.00	21.00	21.00	
Zr	380	410	512	390	401	375	330	218	255	260	293	324	400	390	570	350
Nb	9.9	11.20	17.4	17	11.8	10.7	24	13.1	8.97	9.3	9.50	13	16	21	21	20
Mo			0.48			0.4		0.72	0.43			0.44				
Cd			0.026			0.026		0.13	0.13			0.13				
In			0.05			0.04		0.052	0.032			0.041				
Sn	4.7		2.29	4.9		2.27	8.1	2.63	1.67	4.0		2.22	2.8	3.6	4.4	4.4
Sb			0.29			0.33		1.46	0.62			0.91				
Cs	2.9	4.50	3.89	4.2	4.70	4.4	7.7	7.1	2.71	1.50	2.60	3.55	3.0	2.5	2.3	3.40
Ba	590	614	566	595	583	551	480	485	212	190	192	300	635	660	620	810
La	32.0	33.7	41.6	34.6	34.3	34.4	38.5	33	26.5	25.0	25.9	34.2	34.0	31.0	39.0	33.1
Ce	74.0	75.2	81.6	74.4	72.0	73.1	84.9	66.9	51.5	51.0	52.4	65.9	77.0	77.0	83.0	74.1
Pr	8.40	8.48	10.1	9.48	8.37	8.08	9.14	7.72	6.18	5.87	6.44	7.88	7.14	6.17	9.55	8.08
Nd	31.4	30.8	39.3	31.6	30.2	30.1	35.2	29.2	24.2	23.2	23.8	30.5	31.7	24.9	33.5	36.0
Sm	5.98	5.98	7.61	5.93	5.78	5.54	6.66	5.78	4.94	4.86	5.00	5.93	5.89	4.59	6.11	6.78
Eu	1.28	1.41	1.54	1.14	1.36	1.19	1.28	1.25	0.86	0.82	0.91	1.08	0.95	0.86	1.12	1.14
Gd	5.09	5.64	6.09	4.38	5.54	4.55	4.98	5.19	4.26	3.39	4.76	5.13	4.00	3.15	4.40	4.52
Tb	0.79	0.79	1	0.70	0.77	0.67	0.92	0.82	0.72	0.62	0.73	0.87	0.63	0.52	0.79	0.88
Dy	4.38	4.28	5.37	4.38	4.29	3.8	5.48	4.86	4.06	3.89	4.35	4.82	3.49	3.22	4.92	5.34
Ho	0.85	0.88	1.08	0.83	0.86	0.76	1.19	1.02	0.84	0.83	0.89	1	0.77	0.69	1.09	1.05
Er	2.39	2.47	2.95	2.37	2.47	2.14	3.24	2.85	2.31	2.34	2.59	2.72	2.12	2.06	3.21	3.07
Tm			0.48			0.34		0.43	0.39			0.44				
Yb	2.41	2.42	3.1	2.00	2.41	2.09	2.85	2.78	2.43	2.36	2.51	2.77	2.17	2.08	2.99	3.15
Lu		0.38	0.48		0.38	0.33		0.43	0.38		0.37	0.44				
Hf	12.0	9.90	13.6	10.0	9.80	9.74	10.1	5.51	6.97	7.3	7.15	9.01	12.2	10.4	20.6	10.8
Ta		1.05	1.31		0.95	0.89		1.01	0.78		0.75	1.09				
W	1.7		1.27	1.2		1.51	2.6	2.35	1.35	1.2		1.66	0.6	1.1	1.1	1.5
Tl	0.54		0.58			0.66	0.22	0.61	0.31			0.42	0.29		0.35	0.33
Pb	12.6		16.2	9.4		15.8	12.00	19.3	12	3.40		13.7	18	12.7	11.0	15
Bi			0.17			0.19		0.32	0.16			0.17				
Th	10.30	13.00	11.7	10.20	11.80	11.7	13.6	11.5	7.6	5.8	8.45	9.85	8.32	6.99	10.0	12.8
U	3.04	3.03	3.42	2.15	2.74	3.1	2.51	2.84	2.57	2.18	2.93	3.02	2.24	1.82	2.58	2.47

Note: Some obviously abnormal data are highlighted. The study of Hu and Gao (2008) analyzed several samples same as those analyzed in Tayl
elements

References:

Chauvel, C. et al., 2014. Constraints from loess on the Hf–Nd isotopic composition of the upper continental crust. Earth and Planetary Science Le

Gallet, S., Jahn, B.-m., Torii, M., 1996. Geochemical characterization of the Luochuan loess-paleosol sequence, China, and paleoclimatic implicat

Gallet, S., Jahn, B.M., Lanoe, B.V., Dia, A., Rossello, E., 1998. Loess geochemistry and its implications for particle origin and composition of the u

Hu, Z., Gao, S., 2008. Upper crustal abundances of trace elements: A revision and update. Chemical Geology, 253(3–4): 205-221.

Jahn, B.M., Gallet, S., Han, J.M., 2001. Geochemistry of the Xining, Xifeng and Jixian sections, Loess Plateau of China: eolian dust provenance a

Taylor, S.R., McLennan, S.M., McCulloch, M.T., 1983. Geochemistry of loess, continental crustal composition and crustal model ages. Geochimic

lor et al. (1983) and Barth et al. (2000). In that case, we presented only data from Hu and Gao (2008), which covered more

etters, 388: 48-58.
tions. Chemical Geology, 133(1–4): 67-88.
upper continental crust. Earth and Planetary Science Letters, 156(3-4): 157-172.
and paleosol evolution during the last 140 ka. Chemical Geology, 178(1-4): 71-94.
ca et Cosmochimica Acta, 47(11): 1897-1905.